

# Principles of Two-Photon Excitation Microscopy and Its Applications to Neuroscience

## Primer

Karel Svoboda<sup>1,\*</sup> and Ryohei Yasuda<sup>2,\*</sup>

<sup>1</sup>HHMI

Cold Spring Harbor Laboratory  
Cold Spring Harbor, New York 11724

<sup>2</sup>Department of Neurobiology  
Duke University Medical Center  
Durham, North Carolina 27710

The brain is complex and dynamic. The spatial scales of interest to the neurobiologist range from individual synapses (~1 μm) to neural circuits (centimeters); the timescales range from the flickering of channels (less than a millisecond) to long-term memory (years). Remarkably, fluorescence microscopy has the potential to revolutionize research on all of these spatial and temporal scales. Two-photon excitation (2PE) laser scanning microscopy allows high-resolution and high-sensitivity fluorescence microscopy in intact neural tissue, which is hostile to traditional forms of microscopy. Over the last 10 years, applications of 2PE, including microscopy and photostimulation, have contributed to our understanding of a broad array of neurobiological phenomena, including the dynamics of single channels in individual synapses and the functional organization of cortical maps. Here we review the principles of 2PE microscopy, highlight recent applications, discuss its limitations, and point to areas for future research and development.

Fluorescence microscopy occupies a unique niche in biological microscopy. Fluorescent objects can be selectively excited and visualized, even in living systems (Lichtman and Conchello, 2005). The sensitivity of fluorescence detection is sufficiently high so that single fluorescent molecules can be detected in the presence of 10<sup>11</sup> nonfluorescent molecules (e.g., water, amino acids, lipids) (Eigen and Rigler, 1994). Chemists have developed myriads of synthetic fluorophores that allow the labeling of cellular structures of interest (Haugland, 1996). Other fluorophores report aspects of cellular function, such as Ca<sup>2+</sup> and Na<sup>+</sup> concentration and membrane potential. The advent of genetically encoded fluorescent proteins (XFPs) allows the tagging of most cellular proteins of interest to measure their spatial distributions and dynamics (Tsien, 1998). XFP-based probes can report a vast range of phenomena that are critical for intracellular signal flow, such as protein-protein interactions and the activation of kinases (Miyawaki, 2005). XFPs also allow the labeling of specific and sparse subpopulations of cells (Feng et al., 2000; Gong et al., 2003; Lendvai et al., 2000). Finally, new modes of microscopy are rapidly expanding the application of fluorescence microscopy to intact tissues (Conchello and Lichtman, 2005; Denk et al., 1990, 1994; Denk and Svoboda, 1997; Helmchen and Denk, 2002, 2005; Lichtman and Conchello, 2005; Mertz,

2004; Zipfel et al., 2003; Jung et al., 2004; Levene et al., 2004).

Fluorescence techniques are well matched to problems in neurobiology. Optical microscopy can resolve single synapses (Cajal, 1995; Muller and Connor, 1991) and track spatially complex dynamics over centimeters of cortical tissue (Grinvald and Hildesheim, 2004). Whenever possible, neurons need to be studied in their natural habitat, and intact brain tissue is an especially challenging place for light microscopy. In wide-field fluorescence microscopy, contrast and resolution are degraded by strong scattering (Denk and Svoboda, 1997). Confocal microscopy can overcome some of the effects of scattering, since the detector pinhole rejects fluorescence from off-focus locations (Conchello and Lichtman, 2005; Denk and Svoboda, 1997). However, scanning a single section excites, and thereby damages, the entire specimen. Furthermore, the pinhole also rejects signal photons emanating from the focus that are scattered on their way out of the tissue. Deep in tissue, confocal microscopy becomes unacceptably wasteful in terms of signal photons (Centonze and White, 1998; Conchello and Lichtman, 2005). Compensating for signal-loss with increased fluorescence excitation leads to phototoxicity and photobleaching. Wide-field and confocal microscopy are thus techniques that are best applied to thin specimens, such as cultured preparations or the most superficial cell layer in a tissue (<20 μm) (Lichtman et al., 1987). Experiments deeper in tissue benefit from two-photon excitation (2PE; also referred to as two-photon, or multiphoton) microscopy, which allows high-resolution and high-contrast fluorescence microscopy deep in the brain (Denk et al., 1994).

2PE microscopy was invented about 15 years ago (Denk et al., 1990). More than one thousand publications have employed, developed, or reviewed 2PE microscopy (Denk and Svoboda, 1997; So et al., 2000; Zipfel et al., 2003; Helmchen and Denk, 2002, 2005). In this Primer, we will follow a brief introduction of the principles of 2PE with a discussion of technical advances and applications to neurobiology. Throughout we will point out the limitations of 2PE microscopy and suggest areas for future development.

### Principles of Two-Photon Excitation Microscopy

Photobleaching and phototoxicity, together referred to as photodamage, limit the application of fluorescence microscopy to living systems. Each excitation event carries the risk of photodamage. Optimizing fluorescence microscopy often means to minimize photodamage by maximizing the probability of detecting a signal photon per excitation event. Compared to other techniques, 2PE microscopy dramatically improves the detection of signal photons per excitation event, especially when imaging deep in highly scattering environments.

In 2PE of fluorescence, two low-energy photons (typically from the same laser) cooperate to cause a higher-energy electronic transition in a fluorescent molecule (Figure 1A). 2PE is a nonlinear process in that the

\*Correspondence: svoboda@cshl.edu (K.S.); yasuda@neuro.duke.edu (R.Y.)

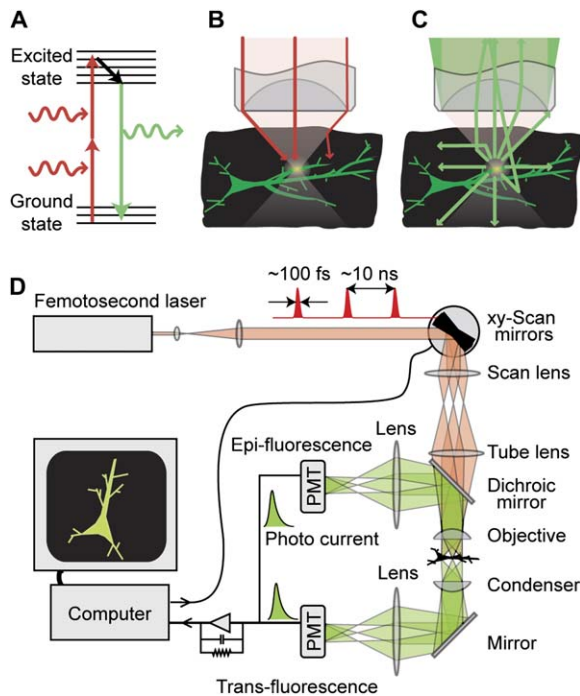


Figure 1. Two-Photon Excitation Microscopy

(A) Simplified Jablonski diagram of the 2PE process. (B) Localization of excitation in a scattering medium (black). The excitation beam (red) is focused to a diffraction-limited spot by an objective where it excites green fluorescence in a dendritic branch, but not in a nearby branch. The paths of two ballistic photons and one scattered photon are shown (red lines). Scattered photons are too dilute to cause off-focus excitation. The intensity of the beam decreases with depth as an increasing number of excitation photons are scattered. (C) Fluorescence collection in a scattering medium. Fluorescence photons are emitted isotropically from the excitation volume (red lines). Even scattered fluorescence photons contribute to the signal if they are collected by the objective. Since the field of view for detection is larger than for excitation, the fluorescence light exiting the objective back-aperture will diverge substantially (green). (D) Schematic of a 2PE microscope with epifluorescence and trans-fluorescence detection.

absorption rate depends on the second power of the light intensity. In a focused laser, the intensity is highest in the vicinity of the focus and drops off quadratically with distance above and below. As a result, fluorophores are excited almost exclusively in a tiny diffraction-limited focal volume (Figure 1B). If the beam is focused by a high numerical aperture (NA) objective, the vast majority of fluorescence excitation occurs in a focal volume that can be as small as  $\sim 0.1 \mu\text{m}^3$  (Zipfel et al., 2003).

The key consequence of localization of excitation is three-dimensional contrast and resolution (comparable to confocal microscopy) without the necessity for spatial filters in the detection path (e.g., the detector pinhole in the confocal microscope) (Wilson and Sheppard, 1984; Denk et al., 1990). To generate an image, the laser is scanned over the specimen. Since the excitation occurs only in the focal volume, all fluorescence photons captured by the microscope objective constitute useful signal. When imaging in thick specimens, the signal yield per excitation event is enhanced (Figure 1B).

The properties of 2PE discussed so far are independent of scattering (Denk et al., 1990). When excitation photons enter tissue, their paths are altered by inhomogeneities in the index of refraction (Denk et al., 1994; Denk and Svoboda, 1997; Helmchen and Denk, 2005). Depending on the type and age of the tissue and the wavelength of the light, about half of the incident photons are scattered every 50–200  $\mu\text{m}$  (Oheim et al., 2001; Yaroslavsky et al., 2002; Kleinfeld et al., 1998). The scattering of excitation light effectively reduces the light delivered to form the diffraction-limited focus (Figure 1B). Scattering also perturbs the trajectories of fluorescence photons on their way out of the tissue (Figure 1C).

Compared to one-photon techniques, 2PE provides three key advantages for microscopy in scattering specimens (Denk et al., 1994). First, the excitation wavelengths used in 2PE microscopy, deep red and near IR, penetrate tissue better than the visible wavelengths used in one-photon microscopy. This improved penetration is due to reduced scattering and reduced absorption by endogenous chromophores (Oheim et al., 2001; Svoboda and Block, 1994; Yaroslavsky et al., 2002). Second, because of the nature of nonlinear excitation, scattered excitation photons are too dilute to cause appreciable fluorescence (Figure 1B). Even deep in tissue, under conditions where most of the incidence photons are scattered, excitation is therefore still mostly limited to a small focal volume (but see the section on depth limitations). Third, because of localization of excitation, all fluorescence photons, ballistic and scattered, constitute useful signal if they are detected (Figure 1B). (In contrast, in wide-field and confocal microscopy, scattered fluorescence photons are either lost, or worse, contribute to background (Gentzone and White, 1998)). Since in typical experiments in tissue the majority of fluorescence photons are scattered, this advantage of two-photon microscopy can be huge.

Since localization of excitation is a direct consequence of the nonlinear nature of 2PE, other nonlinear contrast mechanisms (Mertz, 2004; Wilson and Sheppard, 1984), including 3PE of fluorescence (Maiti et al., 1997) and second harmonic generation (Campagnola et al., 1999; Gannaway and Sheppard, 1978), can be used for optical sectioning microscopy. 3PE may be useful to study endogenous tissue chromophores with one-photon spectra in the UV (Maiti et al., 1997; Zipfel et al., 2003). Second harmonic generation can selectively excite probes that are aligned at interfaces and may therefore be useful to study the structure and function of membranes (Moreaux et al., 2000; Dombeck et al., 2004).

#### Hardware and Software

2PE microscopy is typically implemented in a simple laser scanning microscope (Figure 1D). A laser is focused to a tight spot in the specimen plane and scanned in a raster over the sample. When the laser focus overlaps with fluorescent molecules in the sample, fluorescence photons are generated selectively in the tiny focal volume and detected by photodetectors. The signals are summed over pixel times (microseconds) and mapped to individual pixels of an image by the data acquisition computer. The simplicity of 2PE microscopes has

allowed numerous labs to adapt confocal microscopes for 2PE microscopy (Majewska et al., 2000b; Nikolenko et al., 2003; Ridsdale et al., 2004). Other labs have opted for complete custom design (Mainen et al., 1999a; Polgruto et al., 2003; Tsai et al., 2002).

The principle differences between confocal and 2PE microscopes are the laser (see below) and the fluorescence detection path. In confocal microscopy, the epifluorescence light passes back through the scan mirrors and through a pinhole before detection (Conchello and Lichtman, 2005). In 2PE microscopy, all fluorescence photons collected by the objective constitute useful signal, and the detector pinhole is not required. The optimal solution for the detection path is to project the objective back-aperture onto the photosensitive area of the photodetector (whole-field detection; Denk et al., 1995a; Mainen et al., 1999a; Tsai et al., 2002) (Figure 1D). Since fluorescence photons may be scattered multiple times before exiting the tissue, they can appear to originate from a large effective field of view (Oheim et al., 2001). Objectives with low magnifications (but maintaining high NA, e.g., 20× 0.9NA) are best for imaging in scattering tissue. However, the back-apertures of these objectives are large, and the scattered fluorescence light exiting the objective diverges rapidly (Oheim et al., 2001). To collect as many fluorescence photons as possible, it is therefore necessary to bring large focusing elements close to the objective back-aperture, which is difficult to implement in commercial microscope stands. Similar considerations apply for transfluorescence collected through the condenser (Mainen et al., 1999a) (Figure 1D).

#### **Lasers**

Because two-photon cross-sections are small, very high instantaneous intensities of excitation light are required to generate sufficient signal levels. 2PE microscopy was made practical (Denk et al., 1990) by the advent of lasers producing rapid trains of short pulses (Gosnell and Taylor, 1991). With the average power and pulse repetition rates constant, the 2PE efficiency increases as the inverse of the pulse duration. Mode-locked Ti:sapphire lasers have nearly ideal properties for 2PE microscopy. They produce a stream of pulses with repetition rates of ~100 MHz; more than 100 pulses impinge on the sample within a typical pixel time, implying that variations in the number of pulses per pixel are small (<1%). The pulse duration produced by turnkey systems is on the order of 100 fs, which may be optimal; shorter pulses would be severely distorted by dispersion in the microscope optics (Guild et al., 1997). Finally, the excitation wavelength is tunable from below 700 nm to above 1000 nm, allowing excitation of most useful fluorophores.

Ti:sapphire lasers perform relatively poorly at wavelengths that are optimal for the excitation of red fluorescent proteins (>1000 nm) (Zipfel et al., 2003). In this wavelength regime, other powerful light sources are available, for example mode-locked Ytterbium-doped lasers (Deguil et al., 2004; Honninger et al., 1998) (fixed wavelength: ranging from 1030 nm to 1060 nm) or Cr:forsterite lasers (Chen et al., 2002a) (tunable, 1200–1300 nm).

#### **Scanners**

The vast majority of laser scanning microscopes use galvanometer mirrors. They have excellent optical properties and allow zooming and image rotation. Their ma-

ior drawback is their relatively slow speed (>1 ms per line); a typical image requires ~1 s. Since many neurophysiological processes occur over milliseconds, faster scanning methods are needed.

In multifocal scanning, the beam is divided into beamlets that are simultaneously scanned across the sample (Andresen et al., 2001; Bewersdorf et al., 1998; Kurtz et al., 2006). This approach demands imaging detectors (i.e., CCDs) since the fluorescence excited by different beamlets needs to be distinguished. In scattering samples, the image will be blurred. In addition, dividing the beam into beamlets with lower power reduces nonlinear excitation.

In highly scattering tissue, point scanning with whole-field detection is preferable. Rapid raster scanning can be performed with rotating polygonal mirrors (Kim et al., 1999) or resonant galvanometers (Fan et al., 1999; Nguyen et al., 2001). These methods have excellent optical properties. However, they have the disadvantage that they are limited to raster scanning with fixed scanning speeds and do not allow zooming or image rotation.

When regions of interest are dispersed sparsely across the sample, raster scanning is slow and wasteful in terms of excitation. In random-access scanning, the beam is directed to predetermined targets in the sample. Galvanometer-mirrors support random-access scanning, but their inertia limits scan speeds to ~1 ms per spot. Acousto-optic deflectors (AOD) offer an attractive alternative. AODs use soundwaves to deflect laser beams, and they can be orders of magnitude faster than galvanometer-mirrors. However, their highly dispersive properties make compromises between excitation efficiency and image quality necessary (Iyer et al., 2003). While picosecond pulses can pass through AODs more or less unaffected, shorter pulses will be temporally and spatially distorted, leading to degradation of the excitation efficiency and the point spread function (Iyer et al., 2006). Temporal dispersion (group velocity dispersion) can be compensated with prism pairs (Iyer et al., 2003; Lechleiter et al., 2002; Roorda et al., 2004), and angular dispersion can be compensated by a prism (Lechleiter et al., 2002; Roorda et al., 2004), grating (Iyer et al., 2003), or another AOD (Ngoi et al., 2001). AODs can also be used to implement lenses for rapid scanning along the optical axis (Kaplan et al., 2001; Reddy and Saggau, 2005). Miniaturization of mechanical scanning systems using microelectromechanical systems (MEMS) technology is promising to provide other versatile approaches to fast scanning in the near future (Flusberg et al., 2005; Wang et al., 2004a).

#### **Objectives**

Objectives are critical for 2PE because they generate the tight laser focus required for localization of excitation. All major microscope manufacturers now produce objectives suitable for 2PE microscopy. Important factors include the NA, which determines resolution and the collection angle for fluorescence; the magnification, which determines the field of view; the working distance; and the efficiency of transmission of the near-IR excitation light.

#### **Detectors**

The optical demands of the detection path limit the choice of photodetectors that are suitable for 2PE

Table 1. Fluorophores and Chromophores for Two-Photon Excitation

| Fluorophores/Chromophores  | $\Phi^a$ (GM) | 2PE <sup>b</sup> (nm)                    | Em. (nm)  | Note   | References  |
|--|---------------|--|-----------|--|---|
| <b>Calcium indicators</b>  |               |  |           |  |   |
| Fluo -3, -4, -5F, 4FF et al.   |               | 810 <sup>c</sup>                         | 520–530   |  | (Yasuda et al., 2004)   |
| Oregon Green BAPTA -1, -2 et al.   |               | 810 <sup>c</sup>                         | 520       |  | (Yasuda et al., 2004)   |
| Calcium green-1 + Ca <sup>2+</sup> ; Calcium green-1 – Ca <sup>2+</sup>      | 30, 2         | 820                                      | 530       |  | (Xu and Webb, 1996; Xu et al., 1996)                              |
| Fura-2 + Ca <sup>2+</sup> ; Fura-2 – Ca <sup>2+</sup>                        | 6, 0.2        | 800                                      | 505       |  | (Wokosin et al., 2004)  |
| Indo-1 + Ca <sup>2+</sup> ; Indo-1 – Ca <sup>2+</sup>                        | 3.5, 1.5      | 700                                      | 400       |  | (Xu and Webb, 1996; Xu et al., 1996)                              |
| <b>Quantum dots</b>  |               |  |           |  |   |
| Quantum dots   | up to 47,000  | broad                                    | variable  |  | (Larson et al., 2003)   |
| <b>Fluorescent proteins</b>  |               |  |           |  |   |
| eCFP   | 100–200       | 800–900                                  | 505       |  | (Zipfel et al., 2003)   |
| eGFP   | 100–200       | 900–1000                                 | 510       |  | (Zipfel et al., 2003)   |
| eYFP   | 100–200       | 930–1000                                 | 530       |  | (Zipfel et al., 2003)   |
| mRFP, mCherry  |               | 1030 <sup>c</sup>                        | 610       | Ytterbium-doped laser                              | (Campbell et al., 2002; Shaner et al., 2004)                      |
| <b>Photoswitchable fluorescent proteins (see also Lukyanov et al., 2005)</b> |               |  |           |  |   |
| paGFP  |               | 750 <sup>g</sup>                         | 515       |  | (Patterson and Lippincott-Schwartz, 2002; Schneider et al., 2005) |
| Kaede  |               | 730 <sup>d</sup>                         | 520 → 580 | green to red; tetramer                             | (Ando et al., 2002)   |
| KFP1   |               | 1120 <sup>d</sup>                        | 600       | tetramer   | (Chudakov et al., 2003)   |
| Dronpa   |               | 780 <sup>d,e</sup> , 1010 <sup>d,f</sup> | 520       | reversible   | (Ando et al., 2004; Habuchi et al., 2005)                         |
| psCFP  |               | 800 <sup>d</sup>                         | 470 → 510 | cyan to green                                      | (Chudakov et al., 2004)   |
| PA-mRFP  |               | 760 <sup>d</sup>                         | 605       |  | (Verkhusha and Sorkin, 2005)                                      |
| KikGR  |               | 760 <sup>c</sup>                         | 520 → 590 | green to red; tetramer                             | (Tsutsui et al., 2005)  |
| Dendra   |               | 960 <sup>d</sup>                         | 505 → 575 | green to red                                       | (Gurskaya et al., 2006)   |
| mEosFP   |               | 780 <sup>d</sup>                         | 520 → 580 | green to red                                       | (Wiedenmann et al., 2004)   |
| <b>Caged glutamate</b>   |               |  |           |  |   |
| MNI-glutamate  | 0.06          | 730                                      |           |  | (Matsuzaki et al., 2001)  |
| <b>Caged calcium</b>   |               |  |           |  |   |
| DM-nitrophen   | 0.013         | 730                                      |           | $K_d$ : 2 nM <sup>h</sup> , 1.5 mM <sup>i</sup>    | (Brown et al., 1999; Momotake et al., 2006)                       |
| Azid-1   | 1.4           | 700                                      |           | $K_d$ : 230 nM <sup>h</sup> , 0.12 mM <sup>i</sup> | (Brown et al., 1999; Momotake et al., 2006)                       |
| NDBF-EGTA  | 0.6           | 710                                      |           | $K_d$ : 14 nM <sup>h</sup> , 1 mM <sup>i</sup>     | (Momotake et al., 2006)   |

<sup>a</sup> Two-photon cross-section, if known.

<sup>b</sup> Wavelength corresponding to the measured two-photon cross-section, unless indicated otherwise.

<sup>c</sup> Wavelength typically used for two-photon excitation.

<sup>d</sup> Wavelength corresponding to twice the peak of one-photon absorption. For fluorescent proteins, this is typically a good estimate of the location of the peak of the two-photon cross-section (Zipfel et al., 2003).

<sup>e</sup> Photoactivation wavelength.

<sup>f</sup> Photoquenching wavelength.

<sup>g</sup> Although its absorption maximum is at 750 nm, we recommend longer wavelength to photo-activate paGFP (e.g., 810 nm). To image paGFP without photoactivating, we use 990 nm (Ti:Sapphire) or 1030 nm (Ytterbium-doped laser).

<sup>h</sup> Affinity for calcium before photolysis.

<sup>i</sup> Affinity for calcium after photolysis.

microscopy. 2PE microscopy requires large photosensitive areas (millimeters) (Oheim et al., 2001), which precludes the use of avalanche photodiodes. Other important factors include the quantum efficiency (QE), gain, absorption spectra, dark noise, and the acceptance angle of the detector. Photomultiplier tubes (PMTs) are best for most applications. The recently developed GaAsP photocathode PMTs (Hamamatsu, H7422P) have improved QE, and short transit time spreads (jitters) which make them useful general purpose detectors, including for fluorescence lifetime imaging (see below). However, their small acceptance angles may lead to signal losses when combined with high-NA/low-magnification objectives.

#### Software

2PE microscope hardware can be assembled mostly with off-the-shelf components. An important component is suitable software to control the microscope and acquire data. Flexible and user-friendly open-source

custom software tools are freely available (Pologru et al., 2003; Tsai et al., 2002; Nguyen et al., 2006).

#### Fluorophores and Chromophores

The photophysical properties of fluorescent probes are critical for experimental design (Table 1). It is difficult to predict 2PE spectra from the one-photon spectra, because different quantum mechanical selection rules apply. The 2PE spectra of several useful fluorescent molecules have been measured (Albota et al., 1998a, 1998b; Xu and Webb, 1996; Xu et al., 1996; Bestvater et al., 2002; Spiess et al., 2005; Fisher et al., 2005; Shear et al., 1997; Wokosin et al., 2004). 2PE cross-sections are expressed in units of Göppert-Mayer (GM  $\equiv 10^{-50}$  cm<sup>4</sup> s). Excellent fluorophores, such as rhodamine B, have cross-sections larger than 100 GM (Xu and Webb, 1996). Bright one-photon fluorophores typically make good two-photon fluorophores, but exceptions have been reported (Xu and Webb, 1996). Compared

to one-photon spectra, two-photon spectra tend to be broader and shifted toward the blue. EGFP, YFP, CFP, and red proteins all have good 2PE cross-sections (Zipfel et al., 2003) ( $\sim 100$  GM). Even some endogenous chromophores can produce usable fluorescence signals under 2PE (Kasischke et al., 2004).

One advantage of the broad 2PE spectra is that a single laser can simultaneously excite multiple fluorescent molecules. The different colors can be separated using dichroic mirrors on the detection side (Xu et al., 1996; Yasuda et al., 2004). This implies that multicolor imaging often requires only a single laser and that the different color images are perfectly aligned.

All fluorescent molecules used in 2PE microscopy so far have been designed with one-photon excitation in mind. Fluorophores optimized for 2PE with very large cross-sections ( $\sim 1000$  GM) have been synthesized (Albota et al., 1998a; Porres et al., 2004). Unfortunately these probes have not yet been successfully used in biological systems.

Semiconductor nanocrystals (quantum dots, QDots) are also promising fluorescent labels for 2PE microscopy. They have broad excitation spectra, narrow emission spectra, and excellent photostability (Fu et al., 2005). QDots are reported to have superb 2PE cross-sections, up to 47,000 GM (Larson et al., 2003). A major challenge in the use of these fluorophores is their large size (hydrodynamic diameter  $\sim 30$  nm; Larson et al., 2003) and their targeting within the specimen.

2PE allows photochemistry in femtoliter volumes (Denk et al., 1990). For example, in combination with suitable caged ligands, 2PE can be used to map the distribution of ligand-gated channels on membranes (photochemical microscopy) (Denk, 1994). However, 2PE uncaging has been limited by the small cross-sections of most available cages. The cross-sections are only appreciable at very short wavelengths ( $\sim 700$  nm), where absorption by endogenous chromophores can result in unacceptable phototoxicity. The time constant of uncaging after absorption is another important factor. Some cages have usable cross-sections, but release is slow after photostimulation so that diffusion destroys the spatial resolution of photochemical microscopy (Furuta et al., 1999). Recently, a flurry of activity in the development of caging chemistry has begun to ameliorate these problems (Brown et al., 1999; DelPrincipe et al., 1999; Kantevari et al., 2006; Kiskin et al., 2002; Klein and Yakel, 2005; Matsuzaki et al., 2001; Momotake et al., 2006; Nikolenko et al., 2005; Niu and Hess, 1993).

Developments of photo-activatable and switchable fluorescence proteins (Ando et al., 2002; Chudakov et al., 2004; Patterson and Lippincott-Schwartz, 2002; Ando et al., 2004; Chudakov et al., 2003; Habuchi et al., 2005; Verkhusha and Sorkin, 2005; Wiedenmann et al., 2004; Tsutsui et al., 2005; Pakhomov et al., 2004; Gurskaya et al., 2006; Lukyanov et al., 2005) allow measurements of protein transport and recycling. 2PE cross-sections of photo-activatable GFP (Patterson and Lippincott-Schwartz, 2002; Schneider et al., 2005) are sufficiently high to visualize proteins in individual spines (Bloodgood and Sabatini, 2005).

Because of the uncertainty principle, trains of short light pulses have broad spectra (Denk et al., 1995a; Gosnell and Taylor, 1991). The dynamic interactions of these

short light pulses with fluorescent molecules are complex and not well understood. Over the last 10 years it has become clear that pulse-shaping, the control of the phases of individual spectral components, can be used to tune a variety of nonlinear processes (Dudovich et al., 2001; Meshulach and Silberberg, 1998). Pulse-shaping can be used to increase the brightness of GFP by a factor of two and, more importantly, reduce photobleaching by a factor of four, while keeping average power constant (Kawano et al., 2003). Similarly, fluorescence excitation in scattering tissue can also be enhanced (Dela Cruz et al., 2004). More work needs to be done to evaluate the exciting opportunities for pulse-shaping in the context of biological 2PE microscopy.

### Photobleaching and Phototoxicity

Photobleaching and phototoxicity play a critical role in biological imaging. It is therefore important to understand photobleaching under conditions typical for 2PE microscopy. In one-photon excitation, the rate of photobleaching is proportional to the rate of fluorescence excitation. The situation is more complicated for 2PE. For several popular fluorophores, including fluorescein and GFP, the bleaching rate increases more rapidly with intensity than the fluorescence intensity (i.e., with an exponent larger than 2) (Patterson and Piston, 2000; Chen et al., 2002b). This indicates that highly labile excited states are accessible by multiphoton absorption (Eggeling et al., 2005).

Multiphoton bleaching has three implications for 2PE microscopy. First, because photobleaching in the focal plane is higher for 2PE than 1PE, 2PE may have little benefit and may even be detrimental for imaging thin samples (i.e., a few focal sections thick). Second, the maximal rate of fluorescence that can be emitted by individual fluorophores is lower with 2PE than with 1PE. Third, the number of fluorescence photons generated before photobleaching depends on the excitation level and the pulse shape. It is therefore not necessarily advantageous to minimize the pulse duration for 2PE microscopy (Koester et al., 1999).

Even less is known about phototoxicity than photobleaching, mainly because measurements of phototoxicity require laborious physiological assays. It is likely that different processes lead to phototoxicity when using different specimens, fluorophores, and excitation wavelengths. Phototoxicity can be mediated by 1PE (Neuman et al., 1999), 2PE (Koester et al., 1999; Konig et al., 1999), or higher-order processes (Hopt and Neher, 2001). In most cases phototoxicity is dominated by excitation of exogenous fluorophores (Koester et al., 1999), but in other situations endogenous chromophores can be more important (Hopt and Neher, 2001; Konig et al., 1999).

### Depth Limitations

Depending on the properties of the tissue (and the exact definition of imaging depth) 2PE microscopy can image up to 1 mm in tissue (Beaurepaire et al., 2001; Theer et al., 2003). Although this is impressive compared to other high-resolution techniques, this depth still covers only a small fraction of the mammalian brain. The imaging depth is determined by scattering: with increasing depth, a smaller fraction of the incidence photons are

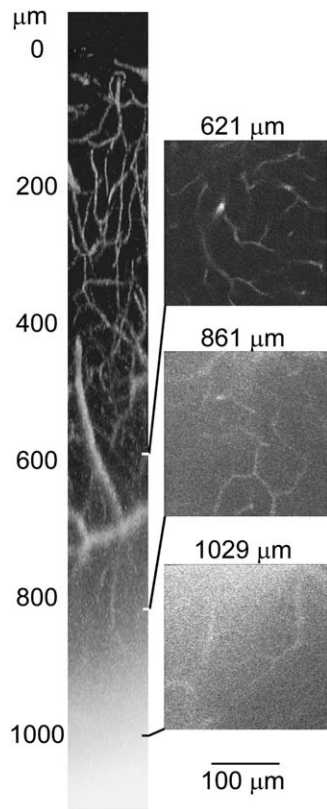


Figure 2. Cerebral Blood Vessels Imaged In Vivo

The vasculature was labeled by injecting fluorescein dextran into the circulatory stream. The light source was a regenerative amplifier. “0 μm” corresponds to the top of the brain. Left, XZ projection. Right, examples of XY projections. Note the increase in background fluorescence deeper than 600 μm in the brain due to out-of-focus 2PE. (Reprinted from Theer et al., 2003, copyright 2003, with permission from the Optical Society of America).

delivered to the focus. Since rays entering the brain at higher angles have longer paths to reach the focus they are more likely to be scattered, causing a loss of resolution with imaging depth. For example, in the mouse neocortex it is possible to image the basal dendrites of L5 pyramidal neurons, but their spines cannot be routinely resolved (unpublished data).

To compensate for scattering, higher laser powers have to be delivered to the sample. Limitations of laser power can be overcome by using more intense light pulses at the expense of repetition rate (Beaurepaire et al., 2001; Theer et al., 2003). However, imaging depth is ultimately limited by fluorescence generated at the surface of the sample by out-of-focus light, which degrades localization of excitation and contrast (Theer et al., 2003) (Figure 2). After this point is reached, increasing laser power or pulse energy further would enhance background and signal equally.

For imaging depths beyond 1 mm, it may be necessary to remove the overlying structures (Mizrahi et al., 2004). Alternatively, fiber-like lenses can be inserted into the brain to image deep structures with excellent resolution (Levene et al., 2004; Flusberg et al., 2005; Jung et al., 2004). In both of these approaches, damage to the structures of interest is a concern.

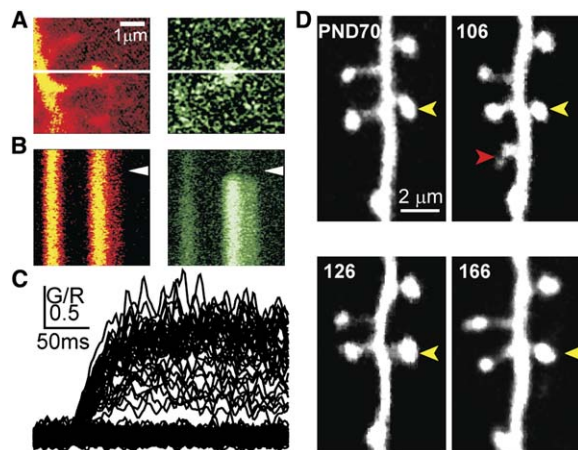


Figure 3. Imaging Small Compartments: Dendritic Spines

(A–C) 2PE microscopy calcium imaging in a neuron loaded with a  $[Ca^{2+}]$  indicator (Fluo-5F; green) and a  $Ca^{2+}$ -insensitive dye (Alexa 594, red). (A) Left, dendrite and spine (red fluorescence). The line indicates the position of the line scan used for (B) and (C). Right,  $[Ca^{2+}]$  transient after synaptic stimulation (green fluorescence,  $\Delta G$ ).

(B) Line scan images.

(C)  $[Ca^{2+}]$  changes after synaptic stimulation measured as the ratio of green/red. Note the clear separation of failures and responses, reflecting the stochastic nature of glutamate release. (Adapted from Oertner et al., 2002, with permission from Nature Publishing Group).

(D) Long-term in vivo imaging of dendrites and spines expressing GFP (A. Holtmaat, unpublished data).

### High-Resolution Imaging in Intact Tissue

The first applications of 2PE microscopy to neurobiology exploited its exquisite resolution in scattering tissue to image the structure and function of dendritic spines in brain slices. 2PE microscopy combined with  $[Ca^{2+}]$  imaging has revealed that spines function as isolated  $Ca^{2+}$  compartments.  $Ca^{2+}$  influx into spines can be dominated by different  $Ca^{2+}$  sources, depending on the physiological stimulus (Yuste and Denk, 1995; Raymond and Redman, 2006; Sabatini et al., 2002; Wang et al., 2000) (Figures 3A–3D). These measurements have further demonstrated that 2PE microscopy-based  $[Ca^{2+}]$  imaging can have sufficient sensitivity to detect the opening of a single  $Ca^{2+}$ -permeable channel (Nimchinsky et al., 2004; Sabatini and Svoboda, 2000; Yasuda et al., 2003b). Similar measurements have been used to analyze the dynamics of  $Ca^{2+}$  in dendrites (Egger et al., 2005; Goldberg et al., 2004; Nevian and Sakmann, 2004; Rozsa et al., 2004) and presynaptic boutons (Cox et al., 2000; Koester and Sakmann, 2000; Rusakov et al., 2004). 2PE microscopy-based  $[Ca^{2+}]$  imaging is an artifact by itself, and the technical details have been discussed elsewhere (Yasuda et al., 2004).

Electrophysiological analysis of synaptic currents has been an invaluable tool to study synaptic transmission (Hestrin et al., 1990), but it has been difficult to isolate the responses of individual synapses. Since there is a one-to-one correspondence between spines and synapses,  $[Ca^{2+}]$  imaging in single spines can be used to study excitatory synaptic transmission at single synapses (Yuste and Denk, 1995; Denk et al., 1995b). This approach has revealed that NMDA receptors are not saturated during low-frequency synaptic transmission (Mainen et al., 1999b) and that the release of glutamate

at single synapses can involve more than one vesicle of glutamate per action potential (Oertner et al., 2002). Measurements of  $\text{Ca}^{2+}$  accumulations mediated by  $\text{Ca}^{2+}$ -permeable AMPARs have been used to dissect the mechanisms underlying synapse-specific signaling in aspiny GABAergic neurons (Soler-Llavina and Sabatini, 2006; Goldberg et al., 2003).

From an imaging perspective, little is different when imaging *in vivo* compared to brain slices. 2PE [ $\text{Ca}^{2+}$ ] imaging has been applied to study the excitation of dendrites in the intact neocortex (Svoboda et al., 1997; Waters and Helmchen, 2004) and the olfactory bulb (Delaney et al., 2001).

The introduction of fluorescent proteins has made new types of experiments possible. XFPs can be delivered to neurons in brain slices and *in vivo* using a variety of noninvasive techniques, including transfection, viral transduction, and transgenesis methods. GFP has been used to image the structure and structural dynamics of dendritic spines in brain slices (Maletic-Savatic et al., 1999; Lang et al., 2004) and *in vivo* (Lendvai et al., 2000). Similarly, the dynamics of GFP-tagged proteins can be imaged with high resolution (Shi et al., 1999; Zito et al., 2004). In transgenic animals expressing XFPs in a subpopulation of neurons, it has been possible to image dendrites and their spines over times of months (Grutzendler et al., 2002; Lee et al., 2005; Mizrahi and Katz, 2003; Trachtenberg et al., 2002; Holtmaat et al., 2004, 2005; Zuo et al., 2005) (Figure 3E). Even thin neocortical axons (diameter  $<100$  nm) can be imaged with high signal-to-noise ratio, not only in adult transgenic mice (De Paola et al., 2006) but even in macaque monkeys (Stettler et al., 2006). These and similar approaches promise to resolve long-standing controversies about structural plasticity in the adult brain and may reveal the cellular correlates of learning and memory.

2PE microscopy is especially well suited for imaging in the retina. Since the retina's photoreceptors are exquisitely sensitive to visible light, they are rapidly bleached by conventional fluorescence microscopy methods. In contrast, the IR light used for 2PE microscopy is not absorbed by photopigments and therefore allows simultaneous functional imaging of retinal neurons and visual stimulation of photoreceptors. 2PE microscopy has been exploited to dissect the mechanisms underlying direction-selectivity in the dendrites of retinal interneurons (Euler et al., 2002; Oesch et al., 2005).

2PE microscopy has also revealed rich dynamism of non-neuronal structures *in vivo*. GFP-labeled microglia, the main immune cells of the brain, show pronounced structural dynamics over tens of seconds and rapidly migrate to sites of brain injury (Davalos et al., 2005; Nimmerjahn et al., 2005). Networks of neocortical astrocytes, bulk-labeled with  $\text{Ca}^{2+}$  indicators, show pronounced [ $\text{Ca}^{2+}$ ] fluctuations that are correlated with the state of the neuronal network (Hirase et al., 2004) and are coupled to vasodilation (Takano et al., 2006). 2PE microscopy of blood flow (Chaigneau et al., 2003; Kleinfeld et al., 1998) has been combined with nonlinear techniques for tissue ablation to study the hemodynamics in response to vascular occlusion (Schaffer et al., 2006). 2PE microscopy can track the structure of thioflavine S-stained senile plaques over time in transgenic mouse models of Alzheimer's disease (Bacskaï et al.,

2001; Christie et al., 2001). In combination with transgenic mice expressing GFP, the effects of plaques on dendritic structure (Tsai et al., 2004) and dendritic spines (Spires et al., 2005) are beginning to be assessed.

#### FRET and Fluorescence Lifetime Measurements

Fluorescence resonance energy transfer (FRET) can be used to image protein-protein interactions in cells. FRET refers to the process of energy transfer from an excited donor fluorophore to an acceptor fluorophore, mediated by dipole-dipole interactions (Förster, 1948). FRET decreases the donor fluorescence and increases the acceptor fluorescence. The efficiency of FRET,  $Y_{\text{FRET}}$ , is the fraction of absorbed photons transferred to the acceptor.  $Y_{\text{FRET}}$  is a steep function of the distance between the fluorophores over distances of  $\sim 5$  nm (Patterson et al., 2000; Selvin, 2000; Yasuda et al., 2003a), and hence FRET reports interactions between proteins fused to fluorophores (Stryer, 1978; Stryer and Haugland, 1967; Uster and Pagano, 1986). FRET can also be used to detect intramolecular conformational changes of proteins tagged with pairs of fluorophores (Clegg et al., 1992; Selvin, 2000; Yasuda et al., 2003a). Numerous protein-protein interactions have been probed with FRET microscopy (Erickson et al., 2001; Miyawaki, 2003; Zacharias et al., 2002). Combining 2PE microscopy with FRET could allow the measurement of biochemical dynamics in neuronal microcompartments within intact neural networks. FRET has been measured using two types of approaches. Intensity measurements at two or more wavelengths can report the quenching of the donor fluorescence and the enhancement of acceptor fluorescence due to FRET (Figure 4). For example, a simple measure of FRET (often used for relative measurements, i.e., before and after a stimulus) is the ratio of donor and acceptor fluorescence,  $D/A$ . This method has been combined with 2PE microscopy (Fan et al., 1999; Okamoto et al., 2004) (Figure 4).

However, interpretation of intensity measurements is complicated by the fact that donor and acceptor absorption and emission spectra overlap (spectral bleed-through) and fluorescence intensities at any wavelength depend on relative concentrations (expression levels). Intensity measurements also fail to distinguish between a small fraction of interacting molecules with high  $Y_{\text{FRET}}$  and a large fraction of interacting molecules with low  $Y_{\text{FRET}}$ . Finally, in scattering tissues  $D/A$  can be further distorted by wavelength-dependent light scattering. Various methods have been devised to deal with spectral bleed-through and fluorophore concentrations (Wallrabe and Periasamy, 2005), but these methods are difficult to combine with 2PE microscopy in intact tissue (Yasuda et al., 2006).

FRET can also be quantified using measurements of the fluorescence lifetime, the average time elapsed between fluorophore excitation and photon emission (Lakowicz, 1999). Fluorescence lifetimes are on the order of nanoseconds. Fluorescence lifetime measurements can be easily combined with 2PE microscopy (2PEFLIM) to provide quantitative FRET imaging (see the legend of Figure 5 for details). These measurements typically involve donor fluorescence only. In the absence of FRET, the donor lifetime is relatively long. FRET cooperates with the usual decay processes to shorten the

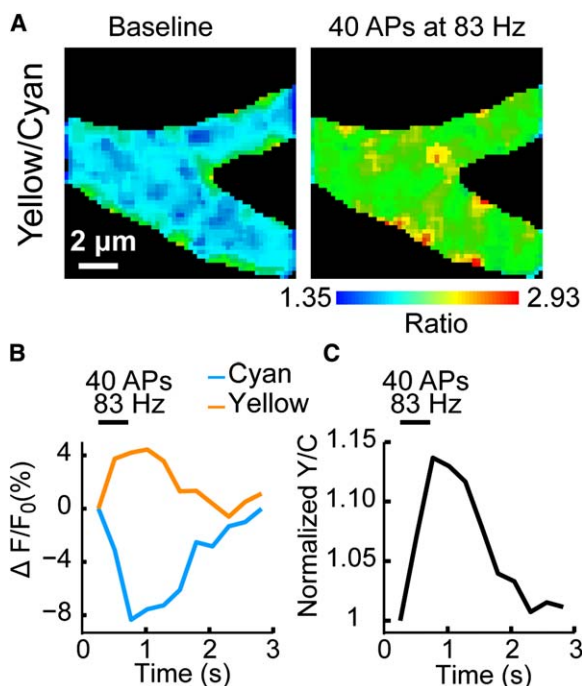


Figure 4. Two-Photon Excitation FRET Measurement

(A) FRET image of a CA1 dendrite expressing Yellow Cameleon 3.6 under baseline conditions and after a train of action potentials. Yellow Cameleon 3.6 (Nagai et al., 2004) was a gift from Atsushi Miyawaki. CFP was excited with a Ti:Sapphire laser running at 810 nm. The emission filters were CFP, 480/40; YFP, 535/50. (B) Time course of cyan and yellow fluorescence. (C) Time course of FRET ratio. (Tianyi Mao and Daniel O'Connor, unpublished data).

fluorescence lifetime. In most biologically relevant situations, where free donors and donors bound to acceptors coexist, the fluorescence decay curve will contain two exponentials. In each pixel, the fluorescence decay curves can be analyzed to derive the fraction of donor interacting with acceptor (binding fraction), perhaps the biologically most meaningful quantity (Figure 5 and legend).

With the help of suitable fluorescent probes, 2PEFLIM with time-correlated single-photon counting can quantify the binding fraction in single dendritic spines (Yasuda et al., 2006) (Figure 5). 2PEFLIM has been used to study the  $[Ca^{2+}]$ -dependent dynamics of Ras in small dendrites and spines (Yasuda et al., 2006). We expect 2PEFLIM to play a prominent role in dissecting neuronal signaling mechanisms in vivo.

### Uncaging and Photochemistry

#### Glutamate and Calcium Uncaging

2PE photolysis of glutamate and  $Ca^{2+}$  can be used to perturb cells with exquisite spatial and temporal resolution (Denk, 1994; Denk et al., 1990). However, applying 2PE photolysis in biologically rich contexts has remained challenging, mainly because the cross-sections of most cages are small and need to be excited at relatively short wavelengths ( $\sim 700$  nm), at which multiphoton absorption by endogenous chromophores produces phototoxicity (Kiskin et al., 2002). Although suitable caged compounds are still rare, the last few years

have seen some notable developments (Table 1). In particular, MNI-caged glutamate provides a sufficiently large 2PE cross-section (0.06 GM) so that glutamate can be photoreleased in synaptic clefts to mimic unitary synaptic currents (Carter and Sabatini, 2004; Matsuzaki et al., 2001; Sobczyk et al., 2005). Stimuli can be repeated sufficiently often to allow fluctuation analysis of glutamate receptors at single synapses. MNI-caged glutamate has facilitated new types of experiments. The number and properties of glutamate receptors in single postsynaptic densities have been measured (Andrasfalvy et al., 2003; Carter and Sabatini, 2004; Matsuzaki et al., 2001; Smith et al., 2003; Sobczyk et al., 2005). Combining 2PE glutamate uncaging with 2PE calcium imaging has allowed the measurement of calcium influx through NMDA receptors and calcium-permeable AMPA receptors in single spines (Carter and Sabatini, 2004; Noguchi et al., 2005; Sobczyk et al., 2005) (Figure 6). 2PE glutamate uncaging has also been used to induce synaptic plasticity in individual spines (Matsuzaki et al., 2004). Stimulation of multiple spines can be used to study the mechanisms of synaptic integration in dendrites (Gasparini and Magee, 2006).

Photolysis of caged calcium can initiate calcium-sensitive signaling in presynaptic (Felmy et al., 2003a; Bollmann et al., 2000; Bollmann and Sakmann, 2005; Schneggenburger and Neher, 2000; Lou et al., 2005; Felmy et al., 2003b) and postsynaptic compartments (Yang et al., 1999) with exquisite spatial and temporal control. Although the development of caged calcium suitable for 2PE is still under development (Brown et al., 1999; Momotake et al., 2006), there have been some attempts to measure the effects of  $[Ca^{2+}]$  increases in astrocytes on cerebrovascular constrictions (Mulligan and MacVicar, 2004). Development of other compounds for 2PE uncaging will advance analyses of molecular processes in neurons at the single synapse level.

#### FRAP and Photoactivation of Fluorescence

To track molecular movements it is necessary to tag the molecules of interest in specific locations. A well-established method is to measure the fluorescence recovery after the photobleaching (FRAP). Using 2PE photobleaching, diffusion of biochemical substances through the spine neck has been measured (Majewska et al., 2000a; Pologruto et al., 2004; Sobczyk et al., 2005; Svoboda et al., 1996; Zito et al., 2004). Inversely, photoactivation of caged fluorophores (Mitchison et al., 1998; Svoboda et al., 1996) and photo-activatable XFPs (Lukyanov et al., 2005) can also be used to measure the diffusion and trafficking of tagged molecules (Bloodgood and Sabatini, 2005) (Figure 7). Photoactivation may offer advantages over FRAP. First, because most photo-activatable fluorescent proteins produce little fluorescence before photo-activation, the measurements have intrinsically higher signal-to-noise ratios: the number of photons required to detect a fluorescence change,  $\Delta F$ , from the baseline fluorescence  $F_0$ , is inversely proportional to  $(\Delta F/F_0)^2$  (Yasuda et al., 2004). Second, photoactivation may produce fewer free radicals and thus induce less phototoxicity.

#### Photoporation

The high peak intensities of light achievable with pulsed lasers have also been used to directly disrupt biological

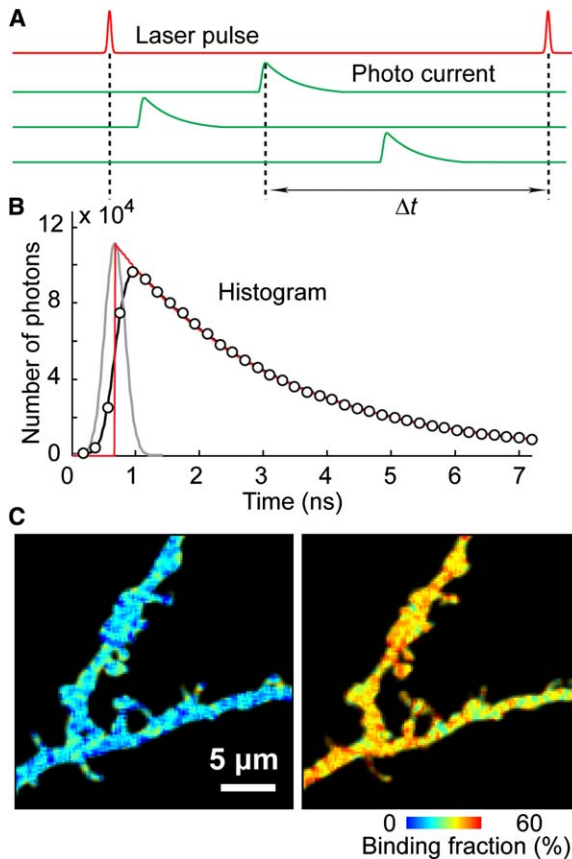


**Figure 5.** Two-Photon Excitation Fluorescence Lifetime Imaging (A) Schematic illustrating the principle of time-correlated photon counting (Becker et al., 2001). The time between photons and the next laser pulse is measured. (B) Measured histogram of photon arrival times (open circles). The curve can be decomposed into the true fluorescence decay curve (red) and a pulse response function (gray) that reflects the finite response time of the detector (Yasuda et al., 2006). (C) 2PEFLIM images of dendrites expressing a FRET sensor for Ras activation before and after membrane depolarization (Yasuda et al., 2006). Each pixel can be expressed as the fraction of Ras bound to acceptor.

Fluorescence lifetime measurements typically involve donor fluorescence only. In the absence of FRET, the time course of the donor fluorescence,  $F$ , after a short pulse of excitation is

$$F = F_0 \exp(-t/\tau_D), \quad (1)$$

where  $\tau_D$  is the fluorescence lifetime of the donor in the absence of acceptor. When FRET occurs, the excited state lifetime of the donor is shortened.

Note that the fluorescence lifetime decreases when FRET occurs. The FRET efficiency, which is defined as the fraction of donor fluorescence quenched by acceptor, can be expressed in measurable quantities simply as

$$Y_{\text{FRET}} = 1 - \tau/\tau_D, \quad (2)$$

where  $\tau$  is the fluorescence lifetime of the donor bound to acceptor. Since only the donor fluorescence is involved, fluorescence lifetime measurements of FRET are independent of fluorophore concentrations and insensitive to wavelength-dependent light scattering. In biologically relevant situations at least two populations of donor co-exist: free donors and donors bound to acceptors. The fluorescence decay curve will contain two exponentials (Lakowicz, 1999):

$$F(t) = F_0 \cdot [P_{\text{AD}} \exp(t/\tau_{\text{AD}}) + P_{\text{D}} \exp(t/\tau_{\text{D}})], \quad (3)$$

where  $P_{\text{AD}}$  and  $P_{\text{D}}$  are the fraction of donor bound and unbound to acceptor, respectively ( $P_{\text{AD}} + P_{\text{D}} = 1$ ).  $P_{\text{AD}}$  is also called the binding

fraction. Illumination with a highly focused beam from a Ti:sapphire laser can cause small, reversible membrane perforations to cause DNA transfection (Tirlapur and König, 2002) or membrane depolarization (Hirase et al., 2002). Larger pulse energies, for example produced by regenerative amplifiers, can be used to perform microsurgery (Nishimura et al., 2006) and sectioning for anatomy (Tsai et al., 2003) down to the level of single axons (Yanik et al., 2004).

### Imaging Neuronal Populations

Single-unit studies employing tungsten microelectrodes have revolutionized our understanding of the functional organization of the brain. However, extracellular recordings have major drawbacks. Only one (or a few) neuron is interrogated at a time, and the cell type and location are not well defined. In addition, only neurons that respond vigorously to the stimulus of interest are usually studied, biasing the sample. 2PE microscopy, in combination with fluorescent probes of neuronal function, has the potential to overcome these problems.

Direct measurement of membrane depolarization can be achieved with voltage-sensitive dyes (Grinvald and Hildesheim, 2004). However, imaging with single-cell resolution has remained challenging except in the most favorable circumstances (Baker et al., 2005). Alternatively, action potentials open voltage-gated calcium channels (VGCCs) and cause  $\text{Ca}^{2+}$  influx into the cytoplasm, which can be readily detected using  $[\text{Ca}^{2+}]$  imaging (Helmchen et al., 1996; Svoboda et al., 1997). Populations of neurons can be loaded with membrane-permeable  $\text{Ca}^{2+}$  indicators in vitro (Yuste et al., 1992) and in vivo (Stosiek et al., 2003). Using these techniques it has been possible to track the dynamics of populations of individual

fraction. Thus, one can derive the fraction of the donor population bound to acceptor from the fluorescence decay curve. It should be noted that sensors for fluorescence lifetime measurements have different design criteria than those for intensity-based methods (Yasuda et al., 2006).

Methods for fluorescence lifetime measurements fall broadly into two groups: time-domain and frequency-domain (Gratton et al., 2003; Lakowicz, 1999). Time-domain methods directly measure the fluorescence decay after a brief excitation pulse. They are typically implemented using time-correlated photon counting (TCSPC) (A), where the timing between laser and photon pulses is measured. This method has high sensitivity, since each photon contributes to the signal. However, because photon counting rates saturate at fairly low levels ( $\sim 10^6$  photons per second) (Becker et al., 2001; Lakowicz, 1999) TCSPC-based imaging may be too slow for some applications (e.g., 1000 photons per histogram in a  $128 \times 128$  pixels image will require  $\sim 15$  s of acquisition time). TCSPC is naturally and easily combined with 2PE since the laser is already pulsed (Becker et al., 2001; Jakobs et al., 2000; Peter et al., 2005; Straub and Hell, 1998). Therefore TCSPC lends itself to high-sensitivity imaging in scattering tissues (Yasuda et al., 2006). Using frequency-domain methods, the fluorescence lifetime is obtained by modulating both excitation intensity and detector gain typically with a sinusoidal function (Philip and Carlsson, 2003; Piston et al., 1992; So et al., 1995; Squire et al., 2000). In contrast to TCSPC, this methods allows unlimited counting rates and thus potentially better temporal resolutions. However, frequency-domain methods are wasteful since only a fraction of detected photons contribute to the signal (Philip and Carlsson, 2003). When measuring fluorescence lifetimes in small subcellular compartments such as dendrites, dendritic spines or axonal boutons (C), the number of photons available is limited and TCSPC methods are preferable (Gratton et al., 2003).

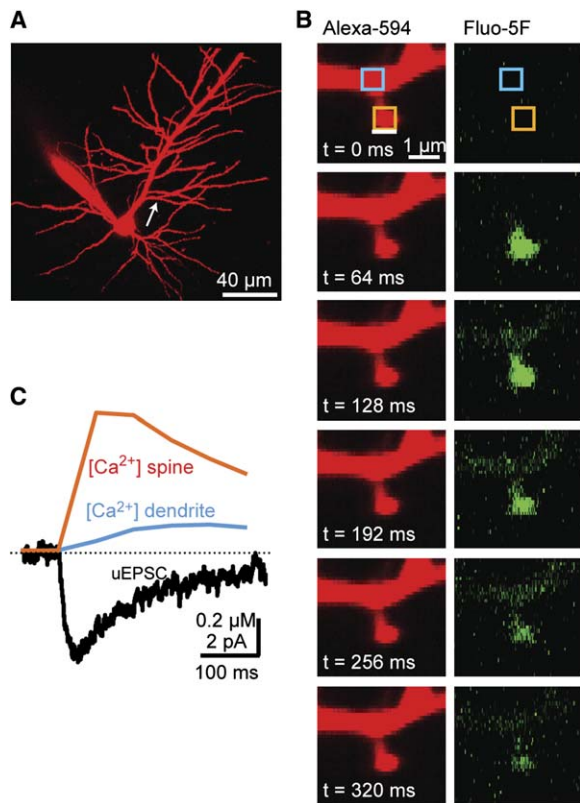


**Figure 6. Simultaneous 2PE Glutamate Uncaging and 2PE Microscopy  $[Ca^{2+}]$  Imaging at Single Spines**  
(A) A neuron loaded with a  $[Ca^{2+}]$  indicator (Fluo-5F; green) and a  $Ca^{2+}$ -insensitive dye (Alexa 594, orange).  
(B) High-magnification time-lapse image of a region of interest (white arrow in [A]). 2PE photolysis of glutamate is indicated by the white bar and occurred immediately after the first image.  
(C) NMDA-receptor-mediated current measured at the soma (black) and changes in calcium concentration (regions of measurement indicated by boxes in [B]).  $\Delta G/R = 1$  corresponds to  $[Ca^{2+}] = 220$  nM. Adapted from Sobczyk et al., 2005.

neurons in vitro (Cossart et al., 2003, 2005) and in vivo (Kerr et al., 2005; Stosiek et al., 2003) (Figure 8). For example,  $[Ca^{2+}]$  imaging can reveal the fine-scale organization of the developing zebrafish tectum (Niell and Smith, 2005), cortical maps in the cat visual cortex (Ohki et al., 2005), and olfactory responses in the zebrafish olfactory bulb (Yaksi and Friedrich, 2006).

A drawback of  $[Ca^{2+}]$  indicators is that it is not straightforward to relate fluorescence changes to number of spikes or spike timing. First, the coupling between activity and  $Ca^{2+}$  accumulations depends on a number of factors that are difficult to control:  $Ca^{2+}$  influx per action potential varies from cell to cell; the  $[Ca^{2+}]$  change depends on the amount of  $[Ca^{2+}]$  indicator trapped in the cell and the size of the compartment imaged;  $Ca^{2+}$  can enter the cell not only through VGCCs but also through synaptic receptors and through calcium-induced calcium release. Second, the relationship between fractional fluorescence changes and  $Ca^{2+}$  accumulations by itself is complex: resting  $Ca^{2+}$  levels vary from cell to cell and compartment to compartment; membrane-permeable forms of  $[Ca^{2+}]$  indicators are often trapped in intracellular compartments, producing

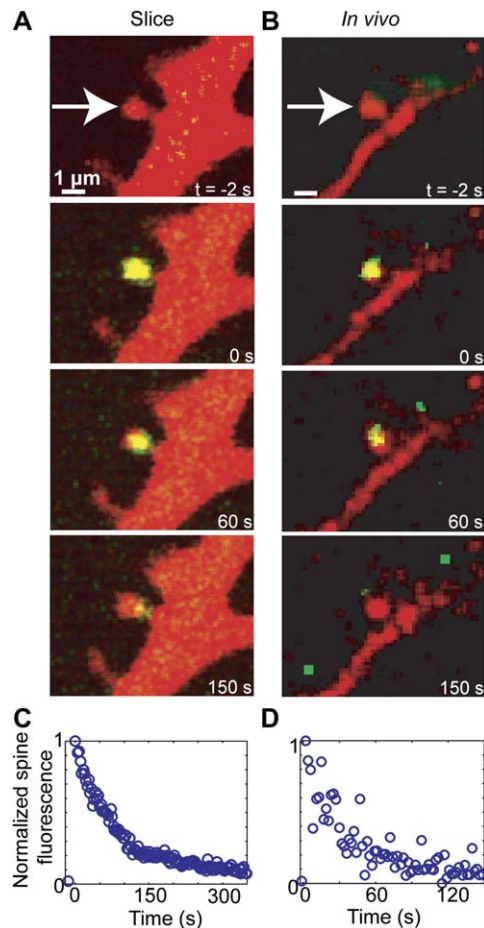


**Figure 7. 2PE Activation of Photoactivatable GFP**  
(A and B) Images of actin tagged with pa-GFP (Patterson and Lippincott-Schwartz, 2002) in a cultured brain slice (A) and in the barrel cortex in vivo (B). Cells were also expressing mCherry (Shaner et al., 2004) as a volume marker. Spines indicated with the arrows were activated using 780 nm light. Imaging was with an Ytterbium-doped laser running at 1030 nm (R. Weimer and N. Gray, unpublished data). (C and D) The time course of green fluorescence in the stimulated spines.

variable static baseline fluorescence;  $Ca^{2+}$  indicators respond sublinearly to  $[Ca^{2+}]$  increases. It is sometimes possible to detect saw-tooth-shaped fluorescence transients corresponding to single spikes (Cossart et al., 2005; Helmchen et al., 1996; Maravall et al., 2000; Svoboda et al., 1997), but the properties of the noise sources in the intact brain may not allow single spike detection reliably in vivo (Kerr et al., 2005; T. Sato and K.S., unpublished observations).

Genetically encoded  $[Ca^{2+}]$  indicators (GECI) may offer an alternative to synthetic indicators. GECIs have been used in combination with 2PE in *Drosophila* (Wang et al., 2003, 2004b) and mice (Hasan et al., 2004). With current GECIs, their slow response kinetics, small dynamic range, and nonlinear behavior only add to the problems discussed for synthetic indicators above (Pologruto et al., 2004). However, progress in indicator development (Diez-Garcia et al., 2005; Guerrero et al., 2005; Mank et al., 2006; Reiff et al., 2005; Palmer et al., 2006; Nagai et al., 2004) and data analysis tools (Yaksi

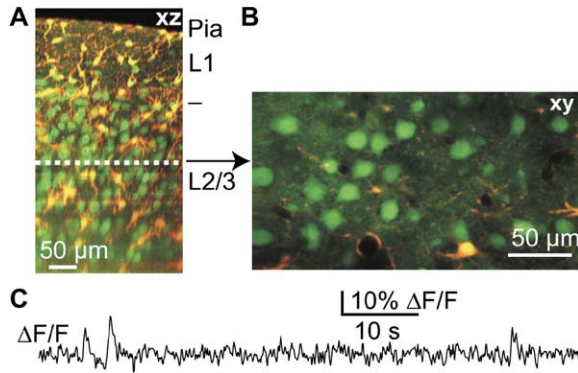


Figure 8. Imaging Neuronal Populations

(A and B) In vivo images of neurons (green, bulk-labeled with Oregon Green Bapta-1 AM) and astrocytes (red-yellow, bulk-labeled with sulforhodamine) (Kerr et al., 2005).

(C) Time course of fluorescence fluctuations in a single neuron.  $[Ca^{2+}]$  transients in response to individual spikes can be detected (Kerr et al., 2005). (Reprinted and modified from Kerr et al., 2005, copyright 2005, National Academy of Sciences, USA).

and Friedrich, 2006) are rapid, and substantial advances can be expected over the next few years.

### Conclusions and Outlook

2PE microscopy is a maturing technology that is contributing to discoveries in neurobiology on many spatio-temporal scales. The limits of 2PE microscopy and the underlying mechanisms are becoming understood. This knowledge is driving technical advances to overcome these limits. 2PE microscopy will continue to benefit from developments in optical physics and optoelectronics. Careful manipulation of the spectral components of the excitation light will allow 2PE microscopy to penetrate deeper in tissue with reduced photodamage (Oron and Silberberg, 2005; Zhu et al., 2005). Adaptive optics may help to compensate for scattering to further improve imaging depth (Feierabend et al., 2004; Neil et al., 2000). A marriage between micromechanical approaches, new fiber optics (Gobel et al., 2004; Ouzounov et al., 2002), and laser scanning microscopy (Wang et al., 2004a) will allow the development of tiny head-mounted 2PE microscopes for imaging in behaving animals, including mice (Flusberg et al., 2005; Helmchen et al., 2001). The development of biocompatible synthetic fluorophores with ultra-large cross-sections would have a profound impact on neuroscience research. It may be possible to mutate or evolve fluorescent proteins for brightness under 2PE (Zacharias and Tsien, 2006). These and other advances will continue to enhance the impact of 2PE microscopy on neuroscience research.

### Acknowledgments

We thank Eric Mottay, Jerome Mertz, and Vijay Iyer for useful discussions; Noah Gray, Anthony Holtmaat, Tianyi Mao, Dan O'Connor, and Robby Weimer for unpublished data; and David Kleinfeld, Chris Harvey, Anthony Holtmaat, Aleks Sobczyk, Linda Wilbrecht, and Haining Zhong for comments on the manuscript. Supported by NIH (K.S.), HHMI (K.S.), Burroughs Wellcome Fund (R.Y.), and the Dana Foundation (R.Y.).

### References

Albota, M., Beljonne, D., Bredas, J.L., Ehrlich, J.E., Fu, J.Y., Heikal, A.A., Hess, S.E., Kogej, T., Levin, M.D., Marder, S.R., et al. (1998a). Design of organic molecules with large two-photon absorption cross sections. *Science* 281, 1653–1656.

Albota, M.A., Xu, C., and Webb, W.W. (1998b). Two-photon fluorescence excitation cross sections of biomolecular probes from 690 to 960 nm. *Appl. Opt.* 37, 7352–7356.

Ando, R., Hama, H., Yamamoto-Hino, M., Mizuno, H., and Miyawaki, A. (2002). An optical marker based on the UV-induced green-to-red photoconversion of a fluorescent protein. *Proc. Natl. Acad. Sci. USA* 99, 12651–12656.

Ando, R., Mizuno, H., and Miyawaki, A. (2004). Regulated fast nucleocytoplasmic shuttling observed by reversible protein highlighting. *Science* 306, 1370–1373.

Andrasfalvy, B.K., Smith, M.A., Borchardt, T., Sprengel, R., and Magee, J.C. (2003). Impaired regulation of synaptic strength in hippocampal neurons from GluR1-deficient mice. *J. Physiol.* 552, 35–45.

Andresen, V., Egner, A., and Hell, S.W. (2001). Time-multiplexed multifocal multiphoton microscope. *Opt. Lett.* 26, 75–77.

Bacskai, B.J., Kajdasz, S.T., Christie, R.H., Carter, C., Games, D., Seubert, P., Schenk, D., and Hyman, B.T. (2001). Imaging of amyloid-beta deposits in brains of living mice permits direct observation of clearance of plaques with immunotherapy. *Nat. Med.* 7, 369–372.

Baker, B.J., Kosmidis, E.K., Vucinic, D., Falk, C.X., Cohen, L.B., Djurisic, M., and Zecevic, D. (2005). Imaging brain activity with voltage- and calcium-sensitive dyes. *Cell. Mol. Neurobiol.* 25, 245–282.

Beaurepaire, E., Oheim, M., and Mertz, J. (2001). Ultra-deep two-photon fluorescence excitation in turbid media. *Opt. Commun.* 188, 25–29.

Becker, W., Bergmann, K., Koenig, K., and Tirlapur, U. (2001). Pico-second fluorescence lifetime microscopy by TCSPC imaging. *Proc SPIE* 4262, 414–419.

Bestvater, F., Spiess, E., Stobrawa, G., Hacker, M., Feurer, T., Porwol, T., Berchner-Pfannschmidt, U., Wotzlaw, C., and Acker, H. (2002). Two-photon fluorescence absorption and emission spectra of dyes relevant for cell imaging. *J. Microsc.* 208, 108–115.

Bewersdorf, J., Pick, R., and Hell, S.W. (1998). Multifocal multiphoton microscopy. *Opt. Lett.* 23, 655–657.

Bloodgood, B.L., and Sabatini, B.L. (2005). Neuronal activity regulates diffusion across the neck of dendritic spines. *Science* 310, 866–869.

Bollmann, J.H., and Sakmann, B. (2005). Control of synaptic strength and timing by the release-site  $Ca^{2+}$  signal. *Nat. Neurosci.* 8, 426–434.

Bollmann, J.H., Sakmann, B., and Borst, J.G. (2000). Calcium sensitivity of glutamate release in a calyx-type terminal. *Science* 289, 953–957.

Brown, E.B., Shear, J.B., Adams, S.R., Tsien, R.Y., and Webb, W.W. (1999). Photolysis of caged calcium in femtoliter volumes using two-photon excitation. *Biophys. J.* 76, 489–499.

Cajal, S.R.y. (1995). *Histology of the Nervous System* (New York: Oxford).

Campagnola, P.J., Wei, M.D., Lewis, A., and Loew, L.M. (1999). High-resolution nonlinear optical imaging of live cells by second harmonic generation. *Biophys. J.* 77, 3341–3349.

Campbell, R.E., Tour, O., Palmer, A.E., Steinbach, P.A., Baird, G.S., Zacharias, D.A., and Tsien, R.Y. (2002). A monomeric red fluorescent protein. *Proc. Natl. Acad. Sci. USA* 99, 7877–7882.

Carter, A.G., and Sabatini, B.L. (2004). State-dependent calcium signaling in dendritic spines of striatal medium spiny neurons. *Neuron* 44, 483–493.

Centonze, V.E., and White, J.G. (1998). Multiphoton excitation provides optical sections from deeper within scattering specimens than confocal imaging. *Biophys. J.* 75, 2015–2024.

Chaigneau, E., Oheim, M., Audinat, E., and Charpak, S. (2003). Two-photon imaging of capillary blood flow in olfactory bulb glomeruli. *Proc. Natl. Acad. Sci. USA* 100, 13081–13086.

- Chen, I.-H., Chu, S.-W., Sun, C.-K., Cheng, P.-C., and Lin, B.-L. (2002a). Wavelength dependent damage in biological multiphoton confocal microscopy: A micro-spectroscopic comparison between femtosecond Ti:sapphire and Cr:forsterite laser sources. *Opt. Quantum Electron.* **34**, 1251–1266.
- Chen, T.S., Zeng, S.Q., Luo, Q.M., Zhang, Z.H., and Zhou, W. (2002b). High-order photobleaching of green fluorescent protein inside live cells in two-photon excitation microscopy. *Biochem. Biophys. Res. Commun.* **291**, 1272–1275.
- Christie, R.H., Bacskai, B.J., Zipfel, W.R., Williams, R.M., Kajdasz, S.T., Webb, W.W., and Hyman, B.T. (2001). Growth arrest of individual senile plaques in a model of Alzheimer's disease observed by in vivo multiphoton microscopy. *J. Neurosci.* **21**, 858–864.
- Chudakov, D.M., Belousov, V.V., Zaraisky, A.G., Novoselov, V.V., Staroverov, D.B., Zorov, D.B., Lukyanov, S., and Lukyanov, K.A. (2003). Kindling fluorescent proteins for precise in vivo photolabeling. *Nat. Biotechnol.* **21**, 191–194.
- Chudakov, D.M., Verkhusha, V.V., Staroverov, D.B., Souslova, E.A., Lukyanov, S., and Lukyanov, K.A. (2004). Photoswitchable cyan fluorescent protein for protein tracking. *Nat. Biotechnol.* **22**, 1435–1439.
- Clegg, R.M., Murchie, A.I., Zechel, A., Carlberg, C., Diekmann, S., and Lilley, D.M. (1992). Fluorescence resonance energy transfer analysis of the structure of the four-way DNA junction. *Biochemistry* **31**, 4846–4856.
- Conchello, J.A., and Lichtman, J.W. (2005). Optical sectioning microscopy. *Nat. Methods* **2**, 920–931.
- Cossart, R., Aronov, D., and Yuste, R. (2003). Attractor dynamics of network UP states in the neocortex. *Nature* **423**, 283–288.
- Cossart, R., Ikegaya, Y., and Yuste, R. (2005). Calcium imaging of cortical networks dynamics. *Cell Calcium* **37**, 451–457.
- Cox, C.L., Denk, W., Tank, D.W., and Svoboda, K. (2000). Action potentials reliably invade axonal arbors of rat neocortical neurons. *Proc. Natl. Acad. Sci. USA* **97**, 9724–9728.
- Davalos, D., Grutzendler, J., Yang, G., Kim, J.V., Zuo, Y., Jung, S., Littman, D.R., Dustin, M.L., and Gan, W.B. (2005). ATP mediates rapid microglial response to local brain injury in vivo. *Nat. Neurosci.* **8**, 752–758.
- De Paola, V., Holtmaat, A., Knott, G., Song, S., Wilbrecht, L., Caroni, P., and Svoboda, K. (2006). Cell-type specific structural plasticity of axonal branches and boutons in the adult neocortex. *Neuron* **49**, 861–875.
- Deguil, N., Mottay, E., Salin, F., Legros, P., and Choquet, D. (2004). Novel Diode-Pumped Infrared Tunable Laser System for Multi-Photon Microscopy. *Microsc. Res. Tech.* **63**, 23–26.
- Dela Cruz, J.M., Pastirk, I., Comstock, M., Lozovoy, V.V., and Dantus, M. (2004). Use of coherent control methods through scattering biological tissue to achieve functional imaging. *Proc. Natl. Acad. Sci. USA* **101**, 16996–17001.
- Delaney, K., Davison, I., and Denk, W. (2001). Odour-evoked [Ca<sup>2+</sup>] transients in mitral cell dendrites of frog olfactory glomeruli. *Eur. J. Neurosci.* **13**, 1658–1672.
- DeiPrincipe, F., Egger, M., Ellis-Davies, G.C., and Niggli, E. (1999). Two-photon and UV-laser flash photolysis of the Ca<sup>2+</sup> cage, dimethoxynitrophenyl-EGTA-4. *Cell Calcium* **25**, 85–91.
- Denk, W. (1994). Two-photon scanning photochemical microscopy: mapping ligand-gated ion channel distributions. *Proc. Natl. Acad. Sci. USA* **91**, 6629–6633.
- Denk, W., and Svoboda, K. (1997). Photon upmanship: why multiphoton imaging is more than a gimmick. *Neuron* **18**, 351–357.
- Denk, W., Strickler, J.H., and Webb, W.W. (1990). Two-photon laser scanning microscopy. *Science* **248**, 73–76.
- Denk, W., Delaney, K.R., Gelperin, A., Kleinfeld, D., Strowbridge, B.W., Tank, D.W., and Yuste, R. (1994). Anatomical and functional imaging of neurons using 2-photon laser scanning microscopy. *J. Neurosci. Methods* **54**, 151–162.
- Denk, W., Piston, D.W., and Webb, W.W. (1995a). Two-photon molecular excitation in laser-scanning microscopy. In *Handbook of Biological Confocal Microscopy*, J.B. Pawley, ed. (New York: Plenum Press), pp. 445–458.
- Denk, W., Sugimori, M., and Llinas, R. (1995b). Two types of calcium response limited to single spines in cerebellar Purkinje cells. *Proc. Natl. Acad. Sci. USA* **92**, 8279–8282.
- Diez-Garcia, J., Matsushita, S., Mutoh, H., Nakai, J., Ohkura, M., Yokoyama, J., Dimitrov, D., and Knopfel, T. (2005). Activation of cerebellar parallel fibers monitored in transgenic mice expressing a fluorescent Ca<sup>2+</sup> indicator protein. *Eur. J. Neurosci.* **22**, 627–635.
- Dombeck, D.A., Blanchard-Desce, M., and Webb, W.W. (2004). Optical recording of action potentials with second-harmonic generation microscopy. *J. Neurosci.* **24**, 999–1003.
- Dudovich, N., Dayan, B., Faeder, S.M.G., and Silberberg, Y. (2001). Transform-limited pulses are not optimal for resonant multiphoton transitions. *Phys. Rev. Lett.* **86**, 47–50.
- Eggeling, C., Volkmer, A., and Seidel, C.A. (2005). Molecular photobleaching kinetics of Rhodamine 6G by one- and two-photon induced confocal fluorescence microscopy. *ChemPhysChem* **6**, 791–804.
- Egger, V., Svoboda, K., and Mainen, Z.F. (2005). Dendrodendritic synaptic signals in olfactory bulb granule cells: local spine boost and global low-threshold spike. *J. Neurosci.* **25**, 3521–3530.
- Eigen, M., and Rigler, R. (1994). Sorting single molecules: applications to diagnostics and evolutionary biotechnology. *Proc. Natl. Acad. Sci. USA* **91**, 5740–5747.
- Erickson, M.G., Alseikhan, B.A., Peterson, B.Z., and Yue, D.T. (2001). Preassociation of calmodulin with voltage-gated Ca(2+) channels revealed by FRET in single living cells. *Neuron* **31**, 973–985.
- Euler, T., Detwiler, P.B., and Denk, W. (2002). Directionally selective calcium signals in dendrites of starburst amacrine cells. *Nature* **418**, 845–852.
- Fan, G.Y., Fujisaki, H., Miyawaki, A., Tsay, R.K., Tsien, R.Y., and Ellisman, M.H. (1999). Video-rate scanning two-photon excitation fluorescence microscopy and ratio imaging with cameleons. *Biophys. J.* **76**, 2412–2420.
- Feierabend, M., Ruckel, M., and Denk, W. (2004). Coherence-gated wave-front sensing in strongly scattering samples. *Opt. Lett.* **29**, 2255–2257.
- Felmy, F., Neher, E., and Schneggenburger, R. (2003a). Probing the intracellular calcium sensitivity of transmitter release during synaptic facilitation. *Neuron* **37**, 801–811.
- Felmy, F., Neher, E., and Schneggenburger, R. (2003b). The timing of phasic transmitter release is Ca<sup>2+</sup>-dependent and lacks a direct influence of presynaptic membrane potential. *Proc. Natl. Acad. Sci. USA* **100**, 15200–15205.
- Feng, G., Mellor, R.H., Bernstein, M., Keller-Peck, C., Nguyen, Q.T., Wallace, M., Nerbonne, J.M., Lichtman, J.W., and Sanes, J.R. (2000). Imaging neuronal subsets in transgenic mice expressing multiple spectral variants of GFP. *Neuron* **28**, 41–51.
- Fisher, J.A., Salzberg, B.M., and Yodanis, A.G. (2005). Near infrared two-photon excitation cross-sections of voltage-sensitive dyes. *J. Neurosci. Methods* **148**, 94–102.
- Flusberg, B.A., Cocker, E.D., Piyawattanametha, W., Jung, J.C., Cheung, E.L., and Schnitzer, M.J. (2005). Fiber-optic fluorescence imaging. *Nat. Methods* **2**, 941–950.
- Förster, V.T. (1948). Zwischenmolekulare Energiewanderung und Fluoresz. *Annalen Dear Physik* **2**, 55–75.
- Fu, A., Gu, W., Larabell, C., and Alivisatos, A.P. (2005). Semiconductor nanocrystals for biological imaging. *Curr. Opin. Neurobiol.* **15**, 568–575.
- Furuta, T., Wang, S.S., Dantzker, J.L., Dore, T.M., Bybee, W.J., Callaway, E.M., Denk, W., and Tsien, R.Y. (1999). Brominated 7-hydroxycoumarin-4-ylmethyls: photolabile protecting groups with biologically useful cross-sections for two photon photolysis. *Proc. Natl. Acad. Sci. USA* **96**, 1193–1200.
- Gannaway, J.N., and Sheppard, C.J.R. (1978). Second-harmonic imaging in the scanning optical microscope. *Opt. Quant. Elect.* **10**, 435–439.
- Gasparini, S., and Magee, J.C. (2006). State-dependent dendritic computation in hippocampal CA1 pyramidal neurons. *J. Neurosci.* **26**, 2088–2100.

- Gobel, W., Nimmerjahn, A., and Helmchen, F. (2004). Distortion-free delivery of nanojoule femtosecond pulses from a Ti:sapphire laser through a hollow-core photonic crystal fiber. *Opt. Lett.* 29, 1285–1287.
- Goldberg, J.H., Tamas, G., Aronov, D., and Yuste, R. (2003). Calcium microdomains in aspiny dendrites. *Neuron* 40, 807–821.
- Goldberg, J.H., Lacefield, C.O., and Yuste, R. (2004). Global dendritic calcium spikes in mouse layer 5 low threshold spiking interneurons: implications for control of pyramidal cell bursting. *J. Physiol.* 558, 465–478.
- Gong, S., Zheng, C., Doughty, M.L., Losos, K., Didkovsky, N., Schambra, U.B., Nowak, N.J., Joyner, A., Leblanc, G., Hatten, M.E., and Heintz, N. (2003). A gene expression atlas of the central nervous system based on bacterial artificial chromosomes. *Nature* 425, 917–925.
- Gosnell, T.R., and Taylor, A.J. (1991). *Selected Papers on Ultrafast Laser Technology* (Bellingham, WA: SPIE Press).
- Gratton, E., Breusegem, S., Sutin, J., Ruan, Q., and Barry, N. (2003). Fluorescence lifetime imaging for the two-photon microscope: time-domain and frequency-domain methods. *J. Biomed. Opt.* 8, 381–390.
- Grinvald, A., and Hildesheim, R. (2004). VSDF: a new era in functional imaging of cortical dynamics. *Nat. Rev. Neurosci.* 5, 874–885.
- Gruzendler, J., Kasthuri, N., and Gan, W.B. (2002). Long-term dendritic spine stability in the adult cortex. *Nature* 420, 812–816.
- Guerrero, G., Reiff, D.F., Agarwal, G., Ball, R.W., Borst, A., Goodman, C.S., and Isacoff, E.Y. (2005). Heterogeneity in synaptic transmission along a *Drosophila* larval motor axon. *Nat. Neurosci.* 8, 1188–1196.
- Guild, J.B., Xu, C., and Webb, W.W. (1997). Measurement of group velocity dispersion of high numerical aperture objective lenses using two-photon excited fluorescence. *Appl. Opt.* 36, 397–401.
- Gurskaya, N.G., Verkhusha, V.V., Shcheglov, A.S., Staroverov, D.B., Chepurmykh, T.V., Fradkov, A.F., Lukyanov, S., and Lukyanov, K.A. (2006). Engineering of a monomeric green-to-red photoactivatable fluorescent protein induced by blue light. *Nat. Biotechnol.* 24, 461–465.
- Habuchi, S., Ando, R., Dedecker, P., Verheijen, W., Mizuno, H., Miyawaki, A., and Hofkens, J. (2005). Reversible single-molecule photo-switching in the GFP-like fluorescent protein Dronpa. *Proc. Natl. Acad. Sci. USA* 102, 9511–9516.
- Hasan, M.T., Friedrich, R.W., Euler, T., Larkum, M.E., Giese, G.G., Both, M., Duebel, J., Waters, J., Bujard, H., Griesbeck, O., et al. (2004). Functional Fluorescent Ca<sup>2+</sup> Indicator Proteins in Transgenic Mice under TET Control. *PLoS Biol.* 2, e163. 10.1371/journal.pbio.0020163.
- Haugland, R.P. (1996). *Handbook of Biological Fluorescent Probes and Research Chemicals*, Sixth edition (Eugene, OR: Molecular Probes).
- Helmchen, F., and Denk, W. (2002). New developments in multiphoton microscopy. *Curr. Opin. Neurobiol.* 12, 593–601.
- Helmchen, F., and Denk, W. (2005). Deep tissue two-photon microscopy. *Nat. Methods* 2, 932–940.
- Helmchen, F., Imoto, K., and Sakmann, B. (1996). Ca<sup>2+</sup> buffering and action potential-evoked Ca<sup>2+</sup> signaling in dendrites of pyramidal neurons. *Biophys. J.* 70, 1069–1081.
- Helmchen, F., Fee, M.S., Tank, D.W., and Denk, W. (2001). A miniature head-mounted two-photon microscope. high-resolution brain imaging in freely moving animals. *Neuron* 31, 903–912.
- Hestrin, S., Nicoll, R.A., Perkel, D.J., and Sah, P. (1990). Analysis of excitatory synaptic action in pyramidal cells using whole-cell recording from rat hippocampal slices. *J. Physiol.* 422, 203–225.
- Hirase, H., Nikolenko, V., Goldberg, J.H., and Yuste, R. (2002). Multiphoton stimulation of neurons. *J. Neurobiol.* 51, 237–247.
- Hirase, H., Qian, L., Bartho, P., and Buzsaki, G. (2004). Calcium dynamics of cortical astrocytic networks in vivo. *PLoS Biol.* 2, e96. 10.1371/journal.pbio.0020096.
- Holtmaat, A.J., Wilbrecht, L., Karpova, A., Portera-Cailliau, C., Burbach, B., Trachtenberg, J.T., and Svoboda, K. (2004). Long-term, high-resolution imaging of neurons in the neocortex in vivo. In *Imaging Neurons*, R. Yuste and A. Konnerth, eds. (Cold Spring Harbor, NY: Cold Spring Harbor Laboratory), pp. 627–638.
- Holtmaat, A.J., Trachtenberg, J.T., Wilbrecht, L., Shepherd, G.M., Zhang, X., Knott, G.W., and Svoboda, K. (2005). Transient and persistent dendritic spines in the neocortex in vivo. *Neuron* 45, 279–291.
- Honninger, C., Morier-Genoud, F., Moser, M., Keller, U., Brovelli, L.R., and Harder, C. (1998). Efficient and tunable diode-pumped femtosecond Yb: glass lasers. *Opt. Lett.* 23, 126–128.
- Hopt, A., and Neher, E. (2001). Highly nonlinear photodamage in two-photon fluorescence microscopy. *Biophys. J.* 80, 2029–2036.
- Iyer, V., Losavio, B.E., and Saggau, P. (2003). Compensation of spatial and temporal dispersion for acousto-optic multiphoton laser-scanning microscopy. *J. Biomed. Opt.* 8, 460–471.
- Iyer, V., Hoogland, T.M., and Saggau, P. (2006). Fast functional imaging of single neurons using random-access multiphoton (RAMP) microscopy. *J. Neurophysiol.* 95, 535–545.
- Jakobs, S., Subramaniam, V., Schonle, A., Jovin, T.M., and Hell, S.W. (2000). EFGP and DsRed expressing cultures of *Escherichia coli* imaged by confocal, two-photon and fluorescence lifetime microscopy. *FEBS Lett.* 479, 131–135.
- Jung, J.C., Mehta, A.D., Aksay, E., Stepnoski, R., and Schnitzer, M.J. (2004). In vivo mammalian brain imaging using one- and two-photon fluorescence microendoscopy. *J. Neurophysiol.* 92, 3121–3133.
- Kantevari, S., Hoang, C.J., Ogronik, J., Egger, M., Niggli, E., and Ellis-Davies, G.C. (2006). Synthesis and two-photon photolysis of 6-(ortho-nitroveratryl)-caged IP3 in living cells. *ChemBioChem* 7, 174–180.
- Kaplan, A., Friedman, N., and Davidson, N. (2001). Acousto-optic lens with very fast focus scanning. *Opt. Lett.* 26, 1078–1080.
- Kasischke, K.A., Vishwasrao, H.D., Fisher, P.J., Zipfel, W.R., and Webb, W.W. (2004). Neural activity triggers neuronal oxidative metabolism followed by astrocytic glycolysis. *Science* 305, 99–103.
- Kawano, H., Nabekawa, Y., Suda, A., Oishi, Y., Mizuno, H., Miyawaki, A., and Midorikawa, K. (2003). Attenuation of photobleaching in two-photon excitation fluorescence from green fluorescent protein with shaped excitation pulses. *Biochem. Biophys. Res. Commun.* 311, 592–596.
- Kerr, J.N., Greenberg, D., and Helmchen, F. (2005). Imaging input and output of neocortical networks in vivo. *Proc. Natl. Acad. Sci. USA* 102, 14063–14068.
- Kim, K.H., Buehler, C., and So, P.T.C. (1999). High-speed, two-photon scanning microscope. *Appl. Opt.* 38, 6004–6009.
- Kiskin, N.I., Chillingworth, R., McCray, J.A., Piston, D., and Ogden, D. (2002). The efficiency of two-photon photolysis of a “caged” fluorophore, o-1-(2-nitrophenyl)ethylpyranine, in relation to photodamage of synaptic terminals. *Eur. Biophys. J.* 30, 588–604.
- Klein, R.C., and Yake, J.L. (2005). Paired-pulse potentiation of alpha7-containing nAChRs in rat hippocampal CA1 stratum radiatum interneurons. *J. Physiol.* 568, 881–889.
- Kleinfeld, D., Mitra, P.P., Helmchen, F., and Denk, W. (1998). Fluctuations and stimulus-induced changes in blood flow observed in individual capillaries in layers 2 through 4 of rat neocortex. *Proc. Natl. Acad. Sci. USA* 95, 15741–15746.
- Koester, H.J., and Sakmann, B. (2000). Calcium dynamics associated with action potentials in single nerve terminals of pyramidal cells in layer 2/3 of the young rat neocortex. *J. Physiol.* 529, 625–646.
- Koester, H.J., Baur, D., Uhl, R., and Hell, S.W. (1999). Ca<sup>2+</sup> fluorescence imaging with pico- and femtosecond two-photon excitation: signal and photodamage. *Biophys. J.* 77, 2226–2236.
- Konig, K., Becker, T.W., Fisher, P., Riemann, I., and Halbhauer, K.J. (1999). Pulse-length dependence of cellular response to intense near-infrared laser pulses in multiphoton microscopes. *Opt. Lett.* 24, 113–115.
- Kurtz, R., Fricke, M., Kalb, J., Tinnefeld, P., and Sauer, M. (2006). Application of multiline two-photon microscopy to functional in vivo imaging. *J. Neurosci. Methods* 151, 276–286.
- Lakowicz, J.R. (1999). *Principles of Fluorescence Spectroscopy*, Second edition (New York: Plenum).

- Lang, C., Barco, A., Zablow, L., Kandel, E.R., Siegelbaum, S.A., and Zakharenko, S.S. (2004). Transient expansion of synaptically connected dendritic spines upon induction of hippocampal long-term potentiation. *Proc. Natl. Acad. Sci. USA* *101*, 16665–16670.
- Larson, D.R., Zipfel, W.R., Williams, R.M., Clark, S.W., Bruchez, M.P., Wise, F.W., and Webb, W.W. (2003). Water-soluble quantum dots for multiphoton fluorescence imaging in vivo. *Science* *300*, 1434–1436.
- Lechleiter, J.D., Lin, D.T., and Sieneart, I. (2002). Multi-photon laser scanning microscopy using an acoustic optical deflector. *Biophys. J.* *83*, 2292–2299.
- Lee, W.C., Huang, H., Feng, G., Sanes, J.R., Brown, E.N., So, P.T., and Nedivi, E. (2005). Dynamic remodeling of dendritic arbors in GABAergic interneurons of adult visual cortex. *PLoS Biol.* *4*, e29. 10.1371/journal.pbio.0040029.
- Lendvai, B., Stern, E., Chen, B., and Svoboda, K. (2000). Experience-dependent plasticity of dendritic spines in the developing rat barrel cortex *in vivo*. *Nature* *404*, 876–881.
- Levene, M.J., Dombeck, D.A., Kasischke, K.A., Molloy, R.P., and Webb, W.W. (2004). *In vivo* multiphoton microscopy of deep brain tissue. *J. Neurophysiol.* *91*, 1908–1912.
- Lichtman, J.W., and Conchello, J.A. (2005). Fluorescence microscopy. *Nat. Methods* *2*, 910–919.
- Lichtman, J.W., Magrassi, L., and Purves, D. (1987). Visualization of neuromuscular junctions over periods of several months in living mice. *J. Neurosci.* *7*, 1215–1222.
- Lou, X., Scheuss, V., and Schneggenburger, R. (2005). Allosteric modulation of the presynaptic Ca<sup>2+</sup> sensor for vesicle fusion. *Nature* *435*, 497–501.
- Lukyanov, K.A., Chudakov, D.M., Lukyanov, S., and Verkhusha, V.V. (2005). Innovation: Photoactivatable fluorescent proteins. *Nat. Rev. Mol. Cell. Biol.* *6*, 885–891.
- Mainen, Z.F., Maletic-Savatic, M., Shi, S.H., Hayashi, Y., Malinow, R., and Svoboda, K. (1999a). Two-photon imaging in living brain slices. *Methods* *18*, 231–239.
- Mainen, Z.F., Malinow, R., and Svoboda, K. (1999b). Synaptic calcium transients in single spines indicate that NMDA receptors are not saturated. *Nature* *399*, 151–155.
- Maiti, S., Shear, J.B., Williams, R.M., Zipfel, W.R., and Webb, W.W. (1997). Measuring serotonin distribution in live cells with three-photon excitation. *Science* *275*, 530–532.
- Majewska, A., Tashiro, A., and Yuste, R. (2000a). Regulation of spine calcium dynamics by rapid spine motility. *J. Neurosci.* *20*, 8262–8268.
- Majewska, A., Yiu, G., and Yuste, R. (2000b). A custom-made two-photon microscope and deconvolution system. *Pflugers Arch.* *441*, 398–408.
- Maletic-Savatic, M., Malinow, R., and Svoboda, K. (1999). Rapid dendritic morphogenesis in CA1 hippocampal dendrites induced by synaptic activity. *Science* *283*, 1923–1927.
- Mank, M., Reiff, D.F., Heim, N., Friedrich, M.W., Borst, A., and Griesbeck, O. (2006). A FRET-based calcium biosensor with fast signal kinetics and high fluorescence change. *Biophys. J.* *90*, 1790–1796.
- Maravall, M., Mainen, Z.M., Sabatini, B.L., and Svoboda, K. (2000). Estimating intracellular calcium concentrations and buffering without wavelength ratiometric. *Biophys. J.* *78*, 2655–2667.
- Matsuzaki, M., Ellis-Davies, G.C., Nemoto, T., Miyashita, Y., Iino, M., and Kasai, H. (2001). Dendritic spine geometry is critical for AMPA receptor expression in hippocampal CA1 pyramidal neurons. *Nat. Neurosci.* *4*, 1086–1092.
- Matsuzaki, M., Honkura, N., Ellis-Davies, G.C., and Kasai, H. (2004). Structural basis of long-term potentiation in single dendritic spines. *Nature* *429*, 761–766.
- Mertz, J. (2004). Nonlinear microscopy: new techniques and applications. *Curr. Opin. Neurobiol.* *14*, 610–616.
- Meshulach, D., and Silberberg, Y. (1998). Coherent quantum control of two-photon transitions by a femtosecond laser pulse. *Nature* *396*, 239–242.
- Mitchison, T.J., Sawin, K.E., Theriot, J.A., Gee, K., and Mallavarapu, A. (1998). Caged fluorescent probes. *Methods Enzymol.* *291*, 63–78.
- Miyawaki, A. (2003). Visualization of the spatial and temporal dynamics of intracellular signaling. *Dev. Cell* *4*, 295–305.
- Miyawaki, A. (2005). Innovations in the imaging of brain functions using fluorescent proteins. *Neuron* *48*, 189–199.
- Mizrahi, A., and Katz, L.C. (2003). Dendritic stability in the adult olfactory bulb. *Nat. Neurosci.* *6*, 1201–1207.
- Mizrahi, A., Crowley, J.C., Shtoyerman, E., and Katz, L.C. (2004). High-resolution *in vivo* imaging of hippocampal dendrites and spines. *J. Neurosci.* *24*, 3147–3151.
- Momotake, A., Lindegger, N., Niggli, E., Barsotti, R.J., and Ellis-Davies, G.C. (2006). The nitroindole chromophore: a new caging group for ultra-efficient photolysis in living cells. *Nat. Methods* *3*, 35–40.
- Moreaux, L., Sandre, O., Blanchard-Desce, M., and Mertz, J. (2000). Membrane imaging by simultaneous second-harmonic generation and two-photon microscopy. *Opt. Lett.* *25*, 320–322.
- Muller, W., and Connor, J.A. (1991). Dendritic spines as individual neuronal compartments for synaptic Ca<sup>2+</sup> responses. *Nature* *354*, 73–76.
- Mulligan, S.J., and MacVicar, B.A. (2004). Calcium transients in astrocyte endfeet cause cerebrovascular constrictions. *Nature* *431*, 195–199.
- Nagai, T., Yamada, S., Tominaga, T., Ichikawa, M., and Miyawaki, A. (2004). Expanded dynamic range of fluorescent indicators for Ca<sup>2+</sup> by circularly permuted yellow fluorescent proteins. *Proc. Natl. Acad. Sci. USA* *101*, 10554–10559.
- Neil, M.A.A., Juskaitis, R., Booth, M.J., Wilson, T., Tanaka, T., and Kawata, S. (2000). Adaptive aberration correction in a two-photon microscope. *J. Microsc.* *200*, 105–108.
- Neuman, K.C., Chadd, E.H., Liou, G.F., Bergman, K., and Block, S.M. (1999). Characterization of photodamage to *Escherichia coli* in optical traps. *Biophys. J.* *77*, 2856–2863.
- Nevian, T., and Sakmann, B. (2004). Single spine Ca<sup>2+</sup> signals evoked by coincident EPSPs and backpropagating action potentials in spiny stellate cells of layer 4 in the juvenile rat somatosensory barrel cortex. *J. Neurosci.* *24*, 1689–1699.
- Ngoi, B.K.A., Venkatakrishnan, K., Lim, L.E.N., and Tan, B. (2001). Angular dispersion compensation for acoustooptic devices used for ultrashort-pulsed laser micromachining. *Opt. Express* *9*, 200–206.
- Nguyen, Q.T., Callamaras, N., Hsieh, C., and Parker, I. (2001). Construction of a two-photon microscope for video-rate Ca<sup>2+</sup> imaging. *Cell Calcium* *30*, 383–393.
- Nguyen, Q.T., Tsai, P.S., and Keinfeld, D. (2006). MPSCOPE: A versatile software suit for multiphoton microscopy. *J. Neurosci. Methods*, in press. Published online April 18, 2006. 10.1016/j.jneumeth.2006.03.001.
- Niell, C.M., and Smith, S.J. (2005). Functional imaging reveals rapid development of visual response properties in the zebrafish tectum. *Neuron* *45*, 941–951.
- Nikolenko, V., Nemet, B., and Yuste, R. (2003). A two-photon and second-harmonic microscope. *Methods* *30*, 3–15.
- Nikolenko, V., Yuste, R., Zayat, L., Baraldo, L.M., and Etchenique, R. (2005). Two-photon uncaging of neurochemicals using inorganic metal complexes. *Chem. Commun. (Camb.)* 1752–1754.
- Nimchinsky, E.A., Yasuda, R., Oertner, T.G., and Svoboda, K. (2004). The number of glutamate receptors opened by synaptic stimulation in single hippocampal spines. *J. Neurosci.* *24*, 2054–2064.
- Nimmerjahn, A., Kirchhoff, F., and Helmchen, F. (2005). Resting microglial cells are highly dynamic surveillants of brain parenchyma *in vivo*. *Science* *308*, 1314–1318.
- Nishimura, N., Schaffer, C.B., Friedman, B., Tsai, P.S., Lyden, P.D., and Kleinfeld, D. (2006). Targeted insult to subsurface cortical blood vessels using ultrashort laser pulses: three models of stroke. *Nat. Methods* *3*, 99–108.
- Niu, L., and Hess, G.P. (1993). An acetylcholine receptor regulatory site in BC3H1 cells: characterized by laser-pulse photolysis in the

- microsecond-to-millisecond time region. *Biochemistry* 32, 3831–3835.
- Noguchi, J., Matsuzaki, M., Ellis-Davies, G.C., and Kasai, H. (2005). Spine-neck geometry determines NMDA receptor-dependent Ca<sup>2+</sup> signaling in dendrites. *Neuron* 46, 609–622.
- Oertner, T.G., Sabatini, B.S., Nimchinsky, E.A., and Svoboda, K. (2002). Facilitation at single synapses probed with optical quantal analysis. *Nat. Neurosci.* 5, 657–664.
- Oesch, N., Euler, T., and Taylor, W.R. (2005). Direction-selective dendritic action potentials in rabbit retina. *Neuron* 47, 739–750.
- Oheim, M., Beaurepaire, E., Chaigneau, E., Mertz, J., and Charpak, S. (2001). Two-photon microscopy in brain tissue: parameters influencing the imaging depth. *J. Neurosci. Methods* 111, 29–37.
- Ohki, K., Chung, S., Ch'ng, Y.H., Kara, P., and Reid, R.C. (2005). Functional imaging with cellular resolution reveals precise microarchitecture in visual cortex. *Nature* 433, 597–603.
- Okamoto, K., Nagai, T., Miyawaki, A., and Hayashi, Y. (2004). Rapid and persistent modulation of actin dynamics regulates postsynaptic reorganization underlying bidirectional plasticity. *Nat. Neurosci.* 7, 1104–1112.
- Oron, D., and Silberberg, Y. (2005). Spatiotemporal coherent control using shaped, temporally focused pulses. *Opt. Express* 13, 9903–9908.
- Ouzounov, D.G., Moll, K.D., Foster, M.A., Zipfel, W.R., Webb, W.W., and Gaeta, A.L. (2002). Delivery of nanojoule femtosecond pulses through large-core microstructured fibers. *Opt. Lett.* 27, 1513–1515.
- Pakhomov, A.A., Martynova, N.Y., Gurskaya, N.G., Balashova, T.A., and Martynov, V.I. (2004). Photoconversion of the chromophore of a fluorescent protein from *Dendronephthya* sp. *Biochemistry (Mosc.)* 69, 901–908.
- Palmer, A.E., Giacomello, M., Kortemme, T., Hires, S.A., Lev-Ram, V., Baker, D., and Tsien, R.Y. (2006). Ca<sup>2+</sup> indicators based on computationally redesigned calmodulin-peptide pairs. *Chem. Biol.*, in press.
- Patterson, G.H., and Lippincott-Schwartz, J. (2002). A photoactivatable GFP for selective photolabeling of proteins and cells. *Science* 297, 1873–1877.
- Patterson, G.H., and Piston, D.W. (2000). Photobleaching in two-photon excitation microscopy. *Biophys. J.* 78, 2159–2162.
- Patterson, G.H., Piston, D.W., and Barisas, B.G. (2000). Forster distances between green fluorescent protein pairs. *Anal. Biochem.* 284, 438–440.
- Peter, M., Ameer-Beg, S.M., Hughes, M.K., Keppler, M.D., Prag, S., Marsh, M., Vojnovic, B., and Ng, T. (2005). Multiphoton-FLIM quantification of the EGFP-mRFP1 FRET pair for localization of membrane receptor-kinase interactions. *Biophys. J.* 88, 1224–1237.
- Philip, J., and Carlsson, K. (2003). Theoretical investigation of the signal-to-noise ratio in fluorescence lifetime imaging. *J. Opt. Soc. Am. A* 20, 368–379.
- Piston, D.W., Sandison, D.R., and Webb, W.W. (1992). Time-resolved fluorescence imaging and background rejection by two-photon excitation in laser-scanning microscopy. In *Time-Resolved Laser Spectroscopy in Biochemistry III*, J.R. Lakowicz, ed. (Bellingham, WA: SPIE), pp. 379–389.
- Pologruto, T.A., Sabatini, B.L., and Svoboda, K. (2003). ScanImage: Flexible software for operating laser-scanning microscopes. *Biomed. Eng. Online* 2, 13.
- Pologruto, T.A., Yasuda, R., and Svoboda, K. (2004). Monitoring neural activity and [Ca<sup>2+</sup>] with genetically encoded Ca<sup>2+</sup> indicators. *J. Neurosci.* 24, 9572–9579.
- Porres, L., Mongin, O., Katan, C., Charlot, M., Bhatthula, B.K.C., Jouikov, V., Pons, T., Mertz, J., and Blanchard-Desce, M. (2004). Two-photon absorption and fluorescence with quadrupolar and branched chromophores - effect of structure and branching. *J. Nonlinear Opt. Phys. Mater.* 13, 451–460.
- Raymond, C.R., and Redman, S.J. (2006). Spatial segregation of neuronal calcium signals encodes different forms of LTP in rat hippocampus. *J. Physiol.* 570, 97–111.
- Reddy, G.D., and Saggau, P. (2005). Fast three-dimensional laser scanning scheme using acousto-optic deflectors. *J. Biomed. Opt.* 10, 64038.
- Reiff, D.F., Ihring, A., Guerrero, G., Isacoff, E.Y., Joesch, M., Nakai, J., and Borst, A. (2005). In vivo performance of genetically encoded indicators of neural activity in flies. *J. Neurosci.* 25, 4766–4778.
- Ridsdale, A., Micu, I., and Stys, P.K. (2004). Conversion of the Nikon C1 confocal laser-scanning head for multiphoton excitation on an upright microscope. *Appl. Opt.* 43, 1669–1675.
- Roorda, R.D., Hohl, T.M., Toledo-Crow, R., and Miesenbock, G. (2004). Video-rate nonlinear microscopy of neuronal membrane dynamics with genetically encoded probes. *J. Neurophysiol.* 92, 609–621.
- Rozsa, B., Zelles, T., Vizi, E.S., and Lendvai, B. (2004). Distance-dependent scaling of calcium transients evoked by backpropagating spikes and synaptic activity in dendrites of hippocampal interneurons. *J. Neurosci.* 24, 661–670.
- Rusakov, D.A., Wuerz, A., and Kullmann, D.M. (2004). Heterogeneity and specificity of presynaptic Ca<sup>2+</sup> current modulation by mGluRs at individual hippocampal synapses. *Cereb. Cortex* 14, 748–758.
- Sabatini, B.L., and Svoboda, K. (2000). Analysis of calcium channels in single spines using optical fluctuation analysis. *Nature* 408, 589–593.
- Sabatini, B.S., Oertner, T.G., and Svoboda, K. (2002). The life-cycle of Ca<sup>2+</sup> ions in spines. *Neuron* 33, 439–452.
- Schaffer, C.B., Friedman, B., Nishimura, N., Schroeder, L.F., Tsai, P.S., Ebner, F.F., Lyden, P.D., and Kleinfeld, D. (2006). Two-photon imaging of cortical surface microvessels reveals a robust redistribution in blood flow after vascular occlusion. *PLoS Biol.* 4, e22. 10.1371/journal.pbio.0040022.
- Schneggenburger, R., and Neher, E. (2000). Intracellular calcium dependence of transmitter release rates at a fast central synapse. *Nature* 406, 889–893.
- Schneider, M., Barozzi, S., Testa, I., Faretta, M., and Diaspro, A. (2005). Two-photon activation and excitation properties of PA-GFP in the 720–920-nm region. *Biophys. J.* 89, 1346–1352.
- Selvin, P.R. (2000). The renaissance of fluorescence resonance energy transfer. *Nat. Struct. Biol.* 7, 730–734.
- Shaner, N.C., Campbell, R.E., Steinbach, P.A., Giepmans, B.N., Palmer, A.E., and Tsien, R.Y. (2004). Improved monomeric red, orange and yellow fluorescent proteins derived from *Discosoma* sp. red fluorescent protein. *Nat. Biotechnol.* 22, 1567–1572.
- Shear, J.B., Xu, C., and Webb, W.W. (1997). Multiphoton-excited visible emission by serotonin solutions. *Photochem. Photobiol.* 65, 931–936.
- Shi, S.H., Hayashi, Y., Petralia, R.S., Zaman, S.H., Wenthold, R.J., Svoboda, K., and Malinow, R. (1999). Rapid spine delivery and redistribution of AMPA receptors after synaptic NMDA receptor activation. *Science* 284, 1811–1816.
- Smith, M.A., Ellis-Davies, G.C., and Magee, J.C. (2003). Mechanism of the distance-dependent scaling of Schaffer collateral synapses in rat CA1 pyramidal neurons. *J. Physiol.* 548, 245–258.
- So, P.T.C., French, T., Yu, W.M., Berland, K.M., Dong, C.Y., and Graton, E. (1995). Time-resolved fluorescence microscopy using two-photon excitation. *Bioimaging* 3, 49–63.
- So, P.T., Dong, C.Y., Masters, B.R., and Berland, K.M. (2000). Two-photon excitation fluorescence microscopy. *Annu. Rev. Biomed. Eng.* 2, 399–429.
- Sobczyk, A., Scheuss, V., and Svoboda, K. (2005). NMDA receptor subunit-dependent [Ca<sup>2+</sup>] signaling in individual hippocampal dendritic spines. *J. Neurosci.* 25, 6037–6046.
- Soler-Llavina, G.J., and Sabatini, B.L. (2006). Synapse-specific plasticity and compartmentalized signaling in cerebellar stellate cells. *Nat. Neurosci.*, in press. Published online May 7, 2006. 10.1038/nn1698.
- Spieß, E., Bestvater, F., Heckel-Pompey, A., Toth, K., Hacker, M., Stobrawa, G., Feuer, T., Wotzlaw, C., Berchner-Pfannschmidt, U., Porwol, T., and Acker, H. (2005). Two-photon excitation and emission spectra of the green fluorescent protein variants ECFP, EGFP and EYFP. *J. Microsc.* 217, 200–204.

- Spires, T.L., Meyer-Luehmann, M., Stern, E.A., McLean, P.J., Skoch, J., Nguyen, P.T., Bacskai, B.J., and Hyman, B.T. (2005). Dendritic spine abnormalities in amyloid precursor protein transgenic mice demonstrated by gene transfer and intravital multiphoton microscopy. *J. Neurosci.* 25, 7278–7287.
- Squire, A., Verveer, P.J., and Bastiaens, P.I. (2000). Multiple frequency fluorescence lifetime imaging microscopy. *J. Microsc.* 197, 136–149.
- Stettler, D.D., Yamahachi, H., Li, W., Denk, W., and Gilbert, C.D. (2006). Dynamic axons and boutons in adult visual cortex. *Neuron* 49, 877–887.
- Stosiek, C., Garaschuk, O., Holthoff, K., and Konnerth, A. (2003). In vivo two-photon calcium imaging of neuronal networks. *Proc. Natl. Acad. Sci. USA* 100, 7319–7324.
- Straub, M., and Hell, S.W. (1998). Fluorescence lifetime three-dimensional microscopy with picosecond precision using a multifocal multiphoton microscope. *Appl. Phys. Lett.* 73, 1769–1771.
- Stryer, L. (1978). Fluorescence energy transfer as a spectroscopic ruler. *Annu. Rev. Biochem.* 47, 819–846.
- Stryer, L., and Haugland, R.P. (1967). Energy transfer: a spectroscopic ruler. *Proc. Natl. Acad. Sci. USA* 58, 719–726.
- Svoboda, K., and Block, S.M. (1994). Biological applications of optical forces. *Annu. Rev. Biophys. Biomol. Struct.* 23, 247–285.
- Svoboda, K., Tank, D.W., and Denk, W. (1996). Direct measurement of coupling between dendritic spines and shafts. *Science* 272, 716–719.
- Svoboda, K., Denk, W., Kleinfeld, D., and Tank, D.W. (1997). In vivo dendritic calcium dynamics in neocortical pyramidal neurons. *Nature* 385, 161–165.
- Takano, T., Tian, G.F., Peng, W., Lou, N., Libionka, W., Han, X., and Nedergaard, M. (2006). Astrocyte-mediated control of cerebral blood flow. *Nat. Neurosci.* 9, 260–267.
- Theer, P., Hasan, M.T., and Denk, W. (2003). Two-photon imaging to a depth of 1000  $\mu\text{m}$  in living brains by use of a Ti:Al<sub>2</sub>O<sub>3</sub> regenerative amplifier. *Opt. Lett.* 28, 1022–1024.
- Tirlapur, U.K., and Konig, K. (2002). Targeted transfection by femtosecond laser. *Nature* 418, 290–291.
- Trachtenberg, J.T., Chen, B.E., Knott, G.W., Feng, G., Sanes, J.R., Welker, E., and Svoboda, K. (2002). Long-term in vivo imaging of experience-dependent synaptic plasticity in adult cortex. *Nature* 420, 788–794.
- Tsai, P.S., Nishimura, N., Yoder, E.J., White, A., Dolnick, E., and Kleinfeld, D. (2002). Principles, design and construction of a two photon scanning microscope for in vitro and in vivo studies. In *Methods for In Vivo Optical Imaging*, R. Frostig, ed. (Boca Raton, FL: CRC Press), pp. 113–171.
- Tsai, P.S., Friedman, B., Ifarraguerrri, A.I., Thompson, B.D., Lev-Ram, V., Schaffer, C.B., Xiong, Q., Tsien, R.Y., Squier, J.A., and Kleinfeld, D. (2003). All-optical histology using ultrashort laser pulses. *Neuron* 39, 27–41.
- Tsai, J., Grutzendler, J., Duff, K., and Gan, W.B. (2004). Fibrillar amyloid deposition leads to local synaptic abnormalities and breakage of neuronal branches. *Nat. Neurosci.* 7, 1181–1183.
- Tsien, R.Y. (1998). The green fluorescent protein. *Annu. Rev. Biochem.* 67, 509–544.
- Tsutsui, H., Karasawa, S., Shimizu, H., Nukina, N., and Miyawaki, A. (2005). Semi-rational engineering of a coral fluorescent protein into an efficient highlighter. *EMBO Rep.* 6, 233–238.
- Uster, P.S., and Pagano, R.E. (1986). Resonance energy transfer microscopy: observations of membrane-bound fluorescent probes in model membranes and in living cells. *J. Cell Biol.* 103, 1221–1234.
- Verkhusha, V.V., and Sorkin, A. (2005). Conversion of the monomeric red fluorescent protein into a photoactivatable probe. *Chem. Biol.* 12, 279–285.
- Wallrabe, H., and Periasamy, A. (2005). Imaging protein molecules using FRET and FLIM microscopy. *Curr. Opin. Biotechnol.* 16, 19–27.
- Wang, S.S., Denk, W., and Hausser, M. (2000). Coincidence detection in single dendritic spines mediated by calcium release. *Nat. Neurosci.* 3, 1266–1273.
- Wang, J.W., Wong, A.M., Flores, J., Vosshall, L.B., and Axel, R. (2003). Two-photon calcium imaging reveals an odor-evoked map of activity in the fly brain. *Cell* 112, 271–282.
- Wang, T.D., Contag, C.H., Mandella, M.J., Chan, N.Y., and Kino, G.S. (2004a). Confocal fluorescence microscope with dual-axis architecture and biaxial postobjective scanning. *J. Biomed. Opt.* 9, 735–742.
- Wang, Y., Guo, H., Pologruto, T.A., Hannan, F., Hakker, I., Svoboda, K., and Zhong, Y. (2004b). Stereotyped odor-evoked activity in the mushroom body of *Drosophila* revealed by green fluorescent protein-based Ca<sup>2+</sup> imaging. *J. Neurosci.* 24, 6507–6514.
- Waters, J., and Helmchen, F. (2004). Boosting of action potential backpropagation by neocortical network activity in vivo. *J. Neurosci.* 24, 11127–11136.
- Wiedenmann, J., Ivanchenko, S., Oswald, F., Schmitt, F., Rocker, C., Salih, A., Spindler, K.D., and Nienhaus, G.U. (2004). EosFP, a fluorescent marker protein with UV-inducible green-to-red fluorescence conversion. *Proc. Natl. Acad. Sci. USA* 101, 15905–15910.
- Wilson, T., and Sheppard, C. (1984). *Theory and Practice of Scanning Optical Microscopy* (New York: Academic Press).
- Wokosin, D.L., Loughrey, C.M., and Smith, G.L. (2004). Characterization of a range of fura dyes with two-photon excitation. *Biophys. J.* 86, 1726–1738.
- Xu, C., and Webb, W.W. (1996). Measurement of two-photon excitation cross sections of molecular fluorophores with data from 690 nm to 1050 nm. *J. Opt. Soc. B* 13, 481–491.
- Xu, C., Zipfel, W., Shear, J.B., Williams, R.M., and Webb, W.W. (1996). Multiphoton fluorescence excitation: new spectral windows for biological nonlinear microscopy. *Proc. Natl. Acad. Sci. USA* 93, 10763–10768.
- Yaksi, E., and Friedrich, R.W. (2006). Reconstruction of firing rate changes across neuronal populations by temporally deconvolved Ca(2+) imaging. *Nat. Methods* 3, 377–383.
- Yang, S.N., Tang, Y.G., and Zucker, R.S. (1999). Selective induction of LTP and LTD by postsynaptic [Ca<sup>2+</sup>]<sub>i</sub> elevation. *J. Neurophysiol.* 81, 781–787.
- Yanik, M.F., Cinar, H., Cinar, H.N., Chisholm, A.D., Jin, Y., and Ben-Yakar, A. (2004). Neurosurgery: functional regeneration after laser axotomy. *Nature* 432, 822.
- Yaroslavsky, A.N., Schulze, P.C., Yaroslavsky, I.V., Schober, R., Ulrich, F., and Schwarzaier, H.J. (2002). Optical properties of selected native and coagulated human brain tissues in vitro in the visible and near infrared spectral range. *Phys. Med. Biol.* 47, 2059–2073.
- Yasuda, R., Masaike, T., Adachi, K., Noji, H., Itoh, H., and Kinoshita, K., Jr. (2003a). The ATP-waiting conformation of rotating F1-ATPase revealed by single-pair fluorescence resonance energy transfer. *Proc. Natl. Acad. Sci. USA* 100, 9314–9318.
- Yasuda, R., Sabatini, B.L., and Svoboda, K. (2003b). Plasticity of calcium channels in dendritic spines. *Nat. Neurosci.* 6, 948–955.
- Yasuda, R., Nimchinsky, E.A., Scheuss, V., Pologruto, T.A., Oertner, T.G., Sabatini, B.L., and Svoboda, K. (2004). Imaging calcium concentration dynamics in small neuronal compartments. *Sci. STKE*, pl5. 10.1126/stke.2192004pl5.
- Yasuda, R., Harvey, C., Zhong, H., Sobczyk, A., and Svoboda, K. (2006). Super-sensitive Ras activation in dendrites and spines revealed by 2-photon fluorescence lifetime imaging. *Nat. Neurosci.* 9, 283–289.
- Yuste, R., and Denk, W. (1995). Dendritic spines as basic functional units of neuronal integration. *Nature* 375, 682–684.
- Yuste, R., Peinado, A., and Katz, L.C. (1992). Neuronal domains in developing neocortex. *Science* 257, 665–669.
- Zacharias, D.A., and Tsien, R.Y. (2006). Molecular biology and mutation of green fluorescent protein. *Methods Biochem. Anal.* 47, 83–120.
- Zacharias, D.A., Violin, J.D., Newton, A.C., and Tsien, R.Y. (2002). Partitioning of lipid-modified monomeric GFPs into membrane microdomains of live cells. *Science* 296, 913–916.

Zhu, G.H., van Howe, J., Durst, M., Zipfel, W., and Xu, C. (2005). Simultaneous spatial and temporal focusing of femtosecond pulses. *Opt. Express* *13*, 2153–2159.

Zipfel, W.R., Williams, R.M., and Webb, W.W. (2003). Nonlinear magic: multiphoton microscopy in the biosciences. *Nat. Biotechnol.* *21*, 1369–1377.

Zito, K., Knott, G., Shepherd, G.M., Shenolikar, S., and Svoboda, K. (2004). Induction of spine growth and synapse formation by regulation of the spine actin cytoskeleton. *Neuron* *44*, 321–334.

Zuo, Y., Lin, A., Chang, P., and Gan, W.B. (2005). Development of long-term dendritic spine stability in diverse regions of cerebral cortex. *Neuron* *46*, 181–189.